A novel form of mouse neutropenia resulting from a point mutation in the zinc finger protein Gfi1

Diana Ordoñez-Rueda[1-3], *Friederike Jönsson[4,5], *David A. Mancardi[4,5], Weidong Zhao[1-3], Aurélie Malzac[1-3], Yinming Liang[1-3], Elodie Bertosio[1-3], Pierre Grenot[1-3], Véronique Blanquet[1-3,9], Sybille Sabrautzki[6], Martin Hrabě de Angelis[6,7], Stéphane Méresse[1-3], Estelle Duprez[8], Pierre Bruhns[4,5], Bernard Malissen[1-3], and Marie Malissen[1-3]

[1]Centre d'Immunologie de Marseille-Luminy, Aix-Marseille Université, Case 906, 13288 Marseille Cedex 9, France

[2]INSERM, U631, 13288 Marseille Cedex 9, France

[3]CNRS, UMR6102, 13288 Marseille Cedex 9, France

[4]Institut Pasteur, Département d'Immunologie, Unité d'Allergologie Moléculaire et Cellulaire, Paris, France

[5]INSERM, U760, Paris, France

[6]Hemholtz Zentrum Muenchen, Institute of Experimental Genetics, Munich, Germany

[7]Lehrstuhl fuer Experimentelle Genetik, Technische Universitaet Muenchen, 85350 Freising-Weihenstephan, Germany

[8]Centre de Recherche en Cancérologie de Marseille (CRCM), Inserm-U1068, Institut Paoli-Calmettes, CNRS-UMR7258, Marseille, France

[9]Present address: UMR1061- Faculté des Sciences et Techniques, Limoges, France.

*F.J. and D.A.M. contributed equally to this study

Short title: A novel form of mouse neutropenia.

Address correspondence to Marie Malissen, Centre d'Immunologie de Marseille-Luminy, Parc Scientifique de Luminy, Case 906, 13288 Marseille, Cedex 09, France.

E-mail address: malissen@ciml.univ-mrs.fr

Phone: 33 4 91 26 94 02; Fax: 33 4 91 26 94 30

Word counts: Text: 5331 words, Abstract: 197 words, 7 Figures, 1 Table, 45 References

Abstract

Using N-ethyl-N-nitrosourea-induced mutagenesis, we established a mouse model with a novel form of neutropenia resulting from a point mutation in the transcriptional repressor Growth Factor Independence 1 (Gfi1). These mice, called *Genista*, had normal viability and no weight loss, in contrast to mice expressing null alleles of the *Gfi1* gene. Further, the *Genista* mutation had a very limited impact on lymphopoiesis or on T and B cell function. Within the bone marrow (BM), the *Genista* mutation resulted in a slight increase of monopoiesis and in a block of terminal granulopoiesis. This block occurred just after the metamyelocytic stage and resulted in the generation of small numbers of atypical $CD11b^{+}Ly\text{-}6G^{int}$ neutrophils, the nuclear morphology of which resembled that of mature WT neutrophils. Unexpectedly, once released from the BM, these atypical neutrophils induced mild forms of autoantibody-induced arthritis and of immune complex-mediated lung alveolitis. They additionally failed to provide resistance to acute bacterial infection. Our study demonstrates that a hypomorphic mutation in the Gfi1 transcriptional repressor results in a novel form of neutropenia characterized by a split pattern of functional responses, reflecting the distinct thresholds required for eliciting neutrophil-mediated inflammatory and anti-infectious responses.

Introduction

Neutrophils contribute to host defense but are also responsible for tissue damage in acute and chronic inflammatory diseases.[1,2] They are short-lived cells that are continuously generated from hematopoietic stem cell (HSC) precursors in the bone marrow (BM) by a process called granulopoiesis.[3] Cells corresponding to sequential stages of granulopoiesis may be characterized by their nuclear shape, cytoplasmic granule content and proliferative status. The earliest granulopoiesis stages correspond to actively dividing cells and are composed of myeloblasts that differentiate into promyelocytes and myelocytes.[4] After exiting the mitotic pool, myelocytes mature into metamyelocytes and then into granulocytes with band-shaped and segmented nuclei. Mature segmented granulocytes contain a heterogeneous population of granules.[5] Upon release into the blood, mature granulocytes are recruited into inflamed tissues in which they contribute to the eradication of invading microbes.[6]

The mechanisms that govern the differentiation of HSCs toward granulocytes rather than monocytes depend on a transcriptional regulatory circuit involving the lineage-determining transcription factors PU.1 and C/EBPα. These factors promote the expression of mutually antagonistic transcriptional repressors.[7,8] Among those antagonistic repressors, growth factor independence 1 (Gfi1) is induced by C/EBPα and is critically required for the development of mature neutrophils. Gfi1 is part of a multi-protein complex that binds DNA and acts as a transcriptional repressor. Gfi1 contains six C_2H_2-type zinc-finger domains and a SNAG domain that is critical for its repressor activity.[8,9] Mice lacking Gfi1 (*Gfi1*$^{-/-}$ mice) showed a severe neutropenia and additional defects in the B and T cell lineages and in the HSC fraction.[10-15] Gfi1 thus controls the development and function of myeloid and lymphoid cells. [16]

Using N-ethyl-N-nitrosourea (ENU)-induced mutagenesis, we have identified and characterized a viable mouse model of neutropenia that resulted from a point mutation in the

Gfi1 gene. Those mice generated small numbers of atypical CD11b^{+}Ly-6G^{int} neutrophils capable of mediating a split pattern of inflammatory and anti-infectious responses.

Materials and Methods

Mice

Mice were housed under specific pathogen free (SPF) conditions and handled in accordance with French and European directives. *Gfi1*$^{-/-}$ and K/BxN mice have been described.[17,18] B6 CD45.1 mice were from Charles River.

ENU mutagenesis screening of mutant mice

The ENU mutagenesis screen was performed in a C57BL/6J (B6; Charles River) background as previously described.[19] Mutant mice were identified as described in the legend of supplemental Figure 1.

Flow cytometry

Stained cells were analyzed using a BD^{TM} LSR II system (BD Biosciences). Data were analyzed with FlowJo software (Tree Star) or FCS Express^{TM} 4, Diva. Cell viability was evaluated using SYTOX Blue (Life technologies). Antibodies used were: APC conjugated anti-CD45.1 (A20), PE Cyc7 conjugated anti-CD19 (1D3), PE Cy5 conjugated anti-CD127 (A7R34), PE conjugated anti-CD16/CD32 (2.4G2), APC conjugated anti-Ly-6C (AL-21) all from BD Pharmingen, PE Cyc7 conjugated anti-CD5 (53-7.3), APC conjugated anti-c-Kit (2B8), PE Cy7 conjugated anti-Sca-1 (D7), FITC conjugated anti-CD34 (RAM34) all from eBioscience, and APC Cyc7 conjugated anti-CD45R (RA3-6B2) and anti-CD3 (145-2C11) from Biolegend.

Western blot analysis

Thymocytes were lysed in Laemmli sample buffer (125 mM Tris-HCl (pH 6.8), 2% SDS, 10% glycerol). Postnuclear supernatants were separated on 8 % SDS-acrylamide gels and

subjected to immunoblot analysis using antibodies against Gfi1 (Santa Cruz Biotechnology) or α-tubulin (Sigma-Aldrich).

Bone marrow chimeras

7-8 week-old B6 (CD45.1) mice were lethally irradiated with two doses of 710 rads, and injected i.v. with 3×10^6 bone marrow (BM) cells isolated from femurs of B6 (CD45.2) or *Genista* (CD45.2) mice. Chimeras were kept on antibiotic-containing water (0.2% Bactrim; Roche) during the whole experiment. 6 weeks after reconstitution, the level of chimerism was determined by staining blood cells for CD45.1 and CD45.2. Mice were killed 8 weeks after reconstitution and $CD45.2^+$ cells from BM, thymus, lymph nodes and spleen were analyzed by flow cytometry.

Quantitative PCR.

Real-time PCR was performed on cDNA samples using following pair of primers were used: *Mpo*: sense 5'- CACACCCTCTTTGTTCGAGA-3', antisense, 5'-CAGGTAGTCCCGGTATGTGA-3', *Ltf*: sense 5'-GTGGAACAGAGCAAGCAGAG-3', antisense, 5'-ACTTGCCCGCAGTGTAGATA-3', *Mmp-9*: sense 5'-CACCACAGCCAACTATGACC-3', antisense, 5'-AGGAAGACGAAGGGGAAGAC-3' and *Hprt*: sense 5'- ATTATGCCGAGGATTTGGAA-3', antisense, 5'-CCCATCTCCTTCATGACATCT-3'. Relative expression values were expressed as 2–ΔcT, where Δ*C*T is the difference between the mean *C*t value of triplicates of the test sample and of the endogenous *Hprt* control.

BrdU incorporation

After receiving a single intra-peritoneal (i.p.) injection of BrdU (1mg per mouse; Sigma), mice were provided with BrdU (3% in drinking water) for 18 hours. Mice were then kept without BrdU for 1, 2 or 3 days. BrdU-labeled cells were detected with a FITC-BrdU flow kit (BD Biosciences).

K/BxN serum-induced passive arthritis

Arthritis was induced by i.v. injection of 70 µl (female) or 80 µl (male) K/BxN serum and arthritis scored as described.[20] Briefly, each paw was graded on a scale 0-3 (leading to a total maximum score of 12) where 0 = no swelling, 1 = swelling confined to one or two digits, or mild swelling of the larger structure, 3= severe arthritis involving the wrist or ankle and 2 = intermediate between 1 and 3. Bioluminescence was measured on an IVIS-100 (Caliper LifeSciences) 5 minutes after injecting mice i.p. with luminol (10 mg/mouse).

Immune complex-mediated lung alveolitis

Mice were injected with 500 µg OVA i.v. and challenged intranasally with 20 µl rabbit anti-OVA antiserum. At different time points after challenge, mice were sacrificed and successive broncho-alveolar lavages (BAL) were performed with PBS. The total numbers of neutrophils and alveolar macrophages recovered from the pooled BAL were determined as described. [21] Hemorrhage was evaluated by measuring OD 570nm (peak of hemoglobin absorption) on pooled BAL treated with a hypotonic buffer. The concentration of total proteins was measured using a Bradford assay (Biorad), that of MMP9 using a ELISA (R&D Systems) and that of TNF-α using a Luminex system (Invitrogen) in the first bronco-alveolar lavage of 0.5ml.

Bacterial peritonitis model

Mice were infected by i.p. injection of 5 x 10^3 CFU of *Salmonella enterica* serovar *typhimurium* 12023 (ATCC 14028) grown in logarithmic phase. Mice were killed after 18 hours of infection and the cells present in the peritoneal cavity were recovered using 5 ml of cold PBS. Viable intracellular bacteria were quantified by determining the number of CFU present in serial dilutions of peritoneal cell lysate prepared with Triton X-100 (0.2 %; Sigma) and plated onto Luria-Bertani agar plates for 18 hours at 37° C.

Survival test

At day 0, 12-week old *Genist*a or B6 female mice were infected by oral gavage using 0.5 x 10^6 CFU of an attenuated *sifA*$^-$ mutant of *S. typhimurium* 12023.[22] Survival was analyzed over a period of 8 days. When specified, mice were subjected to neutrophil depletion by injecting i.v. 100 µg of anti-Gr-1 antibody (RB6-C85; BioXcell, USA) at day -1 and 2.

Statistical analysis

The unpaired Student *t* test was used for statistical analyses with GraphPad Prism software. The *p* values were calculated by t test: **p,* ≤0.05, ***p*, ≤0.01, and ****p*, ≤0.001. All data are presented as the arithmetic mean ± SEM.

Results

The *Genista* phenotype

We conducted a ENU mutagenesis screen on mice of C57BL/6J (B6) background to identify mutations affecting hematopoietic cell development. By determining the absolute numbers of myeloid and lymphoid cells in the blood of G3 offspring (supplemental Figure 1), we identified a neutropenic mutant mouse that is denoted as *Genista* (Figure 1A and supplemental Figure 1). In WT mice, mature neutrophils express high levels of CD11b and Ly-6G molecules. The blood of *Genista* mice was devoid of CD11b$^+$Ly-6G^{high} neutrophils and instead contained an atypical population of CD11b$^+$Ly-6G^{int} cells that were 7-fold less numerous than the CD11b$^+$Ly-6G^{high} neutrophils found in WT blood and the nuclear morphology of which resembled mature WT neutrophils (Figure 1B and data not shown). The blood of *Gfi1*$^{-/-}$ mice also lacked mature Ly-6G^{high} neutrophils but differed from that of *Genista* mice in that it did not contain atypical CD11b$^+$Ly-6G^{int} cells (Figure 1C). *Genista* mice showed a slight increase in the number of Ly-6C^{high} and Ly-6C^{low} blood monocytes (Figure 1A-B and data not shown). A similar trend has been reported for *Gfi1*$^{-/-}$ mice.[11,12,14] Finally, the numbers of eosinophils and of T and B cells found in the blood were not significantly altered in *Genista* mutant mice (Figure 1B). Importantly, the *Genista* mice

differed from *Gfi1*$^{-/-}$ mice in that they showed a normal survival rate and no weight loss, and did not require to be kept under long-term antibiotic treatment.[23]

Characterization of the *Genista* mutation

The *Genista* mutation was inherited in a recessive Mendelian fashion and was mapped by outcrossing *Genista* mice to C3HeB/FeJ (C3H) mice. Following brother-sister mating, 46 neutropenic offspring were identified and subsequently genotyped with a panel of 153 single nucleotide polymorphism (SNP) markers, revealing a linkage to chromosome 5 (Figure 2A). The highest -log10(P) value was associated with SNP rs32067291 that corresponded to position 111.71 of chromosome 5 (chromosomal coordinates are according to http://mouse.ensembl..org/). High-resolution haplotype mapping performed around position 111.71 with 8 additional SNP markers indicated that the *Genista* mutation was localized in the 106.2 - 124.91 interval of chromosome 5 (Figure 2B). Direct genomic sequencing covering splice sites and exons identified a single base change in exon 6 of the *Gfi1* gene present in *Genista* mice, where a G → A transition occurred at position 1081492165 of chromosome 5 (Figure 2C). The *Genista* mutation (C57BL/6-*Gfi1*$^{Gen\ tm1Mal)}$ converted the cysteine (C) residue normally found at position 318 of the third zinc finger domain of Gfi1 into a tyrosine (Y), thereby disrupting the Cys_2His_2 structural motif that constitutes the core component of zinc finger domains (Figure 2 D and E). Importantly, the C318Y substitution present in *Genista* mice had no impact on the levels of expression of the mutated Gfi1^{C318Y} protein as determined by immunoblot analysis of thymocytes (Figure 1D).

Lymphoid cell development and function in *Genista* mice

We analyzed next whether *Genista* mice resembled *Gfi1*$^{-/-}$ mice and showed defects in T and B cell development and function. T cells develop in the thymus through discrete stages defined on the basis of CD4 and CD8 expression. Immature double-negative (DN) $CD4^-CD8^-$ T cells give rise to double-positive (DP) $CD4^+CD8^+$ cells. DP cells further mature into single-

positive (SP) $CD4^+CD8^-$ and $CD4^-CD8^+$ cells that subsequently egress to the periphery. The cellularity of *Genista* thymi was two-fold reduced as compared to WT thymi (Table 1). However, all stages of thymic T cell development were properly represented (Table 1 and supplemental Figure 2). Therefore, the *Genista* thymus is likely colonized by reduced numbers of T cell precursors that then undergo a proper developmental sequence. The secondary lymphoid organs of *Genista* and WT mice contained identical T cell numbers and showed a normal distribution of $CD4^+$, $CD8^+$ and $Foxp3^+$ T cells (Table 1). Peripheral $CD4^+$ and $CD8^+$ T cells of *Genista* mice showed respectively a 1.3- and 3-fold increase in the percentage of cells with a "memory-like" $CD62L^-CD44^{high}$ phenotype (Supplemental Figure 2). Such an increase in the frequency of memory-like T cells may result from the compensatory lymphopenia-driven cell proliferation that frequently occurs in mutant mice with inefficient thymopoiesis.[24] When activated with anti-CD3 plus anti-CD28 antibody, $CD4^+$ and $CD8^+$ T cells of *Genista* and of WT mice showed identical rates of proliferation (data not shown). The *Genista* mutation had no effect on Th1 and Th2 polarization *in vitro* (data not shown).

Early B cell development occurs in the BM and can be separated into several stages.[25]. Although *Genista* mice showed a two-fold reduction in the absolute numbers of cells belonging to the earliest stages of B cell development (denoted as fractions A and B in Table 1), subsequent development was not affected by the *Genista* mutation, thereby resulting in normal numbers of peripheral B cells. When stimulated with anti-IgM antibody and IL-4, peripheral B cells from *Genista* mice showed normal proliferative responses and the serum of *Genista* mice contained normal concentrations of Ig isotypes (data not shown). Therefore, the *Genista* mutation differed from null alleles of the *Gfi1* gene,[11,12,14,15] in that it had a very limited impact on lymphopoiesis and on T and B cell functionality.

Myeloid cell development in *Genista* mice

Congruent with observations of blood, the BM of *Genista* mice lacked $CD11b^{+}Ly\text{-}6G^{high}$ mature neutrophils (Figure 3A and Table 1). The number of monocytes found in *Genista* BM was increased 4-fold as compared to WT BM (Figure 3A and B and Table 1). The dendritic cell (DC) subsets characteristic of secondary lymphoid tissues and of non lymphoid tissues such as the skin were present in normal numbers in *Genista* mice (Table 1 and data not shown). Therefore, within the myeloid lineage, the *Genista* mutation resulted only in a block of granulopoiesis and in a slight increase in BM monopoiesis.

Hematopoietic progenitors and reconstitution capacity of *Genista* bone marrow

HSC can give rise to common lymphoid progenitors (CLP) and to common myeloid progenitors (CMP). CMP are able to further generate megakaryocyte-erythrocyte progenitors (MEP) and granulocyte-monocyte progenitors (GMP). Analysis of the hematopoietic precursor populations isolated from *Genista* BM only revealed a two-fold increase in the numbers of GMP (supplemental Figure 3 and Table 1). The BM from *Gfi1*$^{-/-}$ mice showed a similar feature but in addition contained dramatically decreased numbers of HSCs and CLPs.[13,18]

We next analyzed the ability of *Genista* BM cells to reconstitute irradiated hosts. Even in the absence of competing BM, a large dose (3×10^{6}) of *Genista* BM cells was needed to rescue the hosts from lethal irradiation (data not shown). Eight weeks after transplantation, the transplanted hosts recapitulated the whole *Genista* phenotype, including neutropenia and the presence of atypical $CD11b^{+}Ly\text{-}6G^{int}$ blood cells (supplemental Figure 4). Therefore, when compared to WT BM cells, *Genista* BM cells had reduced reconstitution capacity. These data suggest that the phenotypic abnormalities observed in *Genista* mice were intrinsic to the hematopoietic precursors and to their derivatives.

Impaired maturation of *Genista* bone marrow neutrophils

Considering that the BM from *Genista* mice contained slightly increased numbers of GMPs and lacked neutrophils expressing mature markers (Figure 3A and supplemental Figure 3), we next determined which stage of granulopoieisis was affected by the *Genista* mutation. When cytospin preparations from total WT BM were analyzed by Wright-Giemsa staining, mature neutrophils were readily distinguishable by their segmented and ring-shaped nuclei (Figure 3C, upper left panel). Consistent with our flow cytometric analysis, mature neutrophils were extremely rare in cytospin preparations from *Genista* BM (Figure 3C, lower left panel). In contrast, myelocytes and metamyelocytes with their distinctive doughnut-shaped nuclei were present in both WT and *Genista* BM (Figure 3C, left panels). These results suggest that in *Genista* BM, the block in the generation of mature neutrophils occurred after the metamyelocytic stage.

Importantly, flow cytometric analysis demonstrated that BM cells from *Genista* mice but not from *Gfi1*$^{-/-}$ mice contained a counterpart of the atypical CD11b^{+}Ly-6G^{int} cells observed in the blood of *Genista* mice. These cells represented less than 4% of total *Genista* BM cells (Figure 3A and supplemental Figure 5). FACS sorting of those CD11b^{+}Ly-6G^{int} BM cells, followed by cytospin and inspection after Wright-Giemsa staining showed that they were heterogeneous. They contained metamyelocytes that were admixed with cells the nuclear morphology of which resembled mature neutrophils (Figure 3C, lower middle panel). When a similar sorting strategy was applied to WT BM cells, CD11b^{+}Ly-6G^{int} cells showed a homogeneous phenotype characteristic of metamyelocytes (Figure 3C, upper middle panel). As expected, the CD11b^{+}Ly-6G^{high} population sorted from WT BM was exclusively composed of mature neutrophils (Figure 3C, upper right panel). The rare *Genista* BM cells in the CD11b^{+}Ly-6G^{high} gate resembled the CD11b^{+}Ly-6G^{int} cells found in the *Genista* BM and were thus not enriched in cells with mature nuclei (Figure 3C, lower right panel). Therefore, the *Genista* mutation blocked terminal granulopoiesis just after the metamyelocytic stage and

resulted in the generation of small numbers of atypical CD11b^{+}Ly-6G^{int} neutrophils that were capable of being released from the BM.

Abnormal granule content in CD11b^{+}Ly-6G^{int} neutrophils from *Genista* mice

Primary granules are produced at the stage of the early promyelocytes, secondary granules in myelocytes and metamyelocytes and tertiary granules are formed in band cells.[5] Therefore, we evaluated *Genista* neutrophils for the expression of transcripts coding for primary (myeloperoxidase; Mpo), secondary (lactoferrin; Ltf) and tertiary (matrix metalloproteinase-9; Mmp9) granule proteins. Accordingly, Lineage^{-}CD11b^{-}Ly-6G^{-} cells containing the earliest stages of granulopoiesis, CD11b^{+}Ly-6G^{int} cells, and CD11b^{+}Ly-6G^{high} mature neutrophils were sorted from the BM of *Genista* and of WT mice. Note that in *Genista* BM, the very small numbers of sorted CD11b^{+}Ly-6G^{high} cells were insufficient for RNA analysis. RNA isolated from each sorted population was subjected to quantitative RT-PCR to determine the relative levels of *Mpo*, *Ltf* and *Mmp9* transcripts (Figure 3D). The CD11b^{+}Ly-6G^{int} fraction found in WT BM was primarily composed of metamyelocytes and, as expected, expressed *Ltf* transcripts and lacked both *Mpo* and *Mmp9* transcripts. The CD11b^{+}Ly-6G^{int} cells found in *Genista* BM lacked *Mpo* transcripts and expressed both *Ltf* and *Mmp9* transcripts (Figure 3D). The expression of *Mmp9* in such CD11b^{+}Ly-6G^{int} cells corroborated our morphological findings indicating that the metamyelocytes that normally constitute the bulk of this fraction in WT mice were admixed with cells that not only resembled mature neutrophils but also expressed *Mmp9*. Therefore, these data suggest that the rare cells that develop beyond the metamyelocyte stage in *Genista* BM had a compound phenotype associating traits characteristic of immature (expression of intermediate levels of Ly-6G) and of mature (*Mmp9* expression, nuclear morphology and the capacity to be released from BM) neutrophils.

Dynamics of neutrophil production in Genista mice

To learn more about the dynamics of neutrophil production in *Genista* mice, proliferating progenitors/precursors were labeled *in vivo* by a single BrdU pulse. Analysis of the BrdU-labeling kinetics of $CD11b^{+}Ly\text{-}6G^{int}$ metamyelocytes and $CD11b^{+}Ly\text{-}6G^{high}$ mature neutrophils found in WT BM showed that they were rapidly labeled (Figure 3 E), a result consistent with the fact that their immediate promyelocyte/myelocyte precursors were actively dividing.[4,8,26,27] Moreover, the delayed labeling observed for $CD11b^{+}Ly\text{-}6G^{high}$ mature granulocytes as compared to $CD11b^{+}Ly\text{-}6G^{int}$ metamyelocytes corresponded to the fact that they are related through a precursor-product relationship. When compared to WT $CD11b^{+}Ly\text{-}6G^{int}$ metamyelocytes, the $CD11b^{+}Ly\text{-}6G^{int}$ cells found in *Genista* BM showed diminished percentages of $BrdU^{+}$ cells at all time points analyzed and a BrdU-labeling kinetics that peaked with a one-day delay as compared to those of WT mice (Figure 3E). These findings suggest that the *Genista* mutation impeded the generation of metamyelocytes and further affected the survival of the atypical $CD11b^{+}Ly\text{-}6G^{int}$ neutrophils. Importantly, the first BrdU-labeled cells appeared in the blood of WT and *Genista* mice 3 days after the onset of labeling (data not shown). Therefore, the release into the circulation of the atypical $CD11b^{+}Ly\text{-}6G^{int}$ neutrophils found in the *Genista* BM occurred with kinetics similar to those of the $CD11b^{+}Ly\text{-}6G^{high}$ mature neutrophils found in WT BM.[28]

Genista mice are not resistant to autoantibody-induced arthritis

Because a few atypical $CD11b^{+}Ly\text{-}6G^{int}$ neutrophils can be released into the circulation of *Genista* mice, we explored whether they are functionally relevant. To test this issue, we used the K/BxN model of autoantibody-induced arthritis.[29] This model is characterized by the presence of autoantibodies to the glycolytic enzyme glucose-6-phosphate isomerase (GPI) and transfer of anti-GPI antibodies or of K/BxN serum sufficed to induce rapid and transient inflammation of distal joints. Affected joints contain infiltrates of myeloid cells involving primarily neutrophils and macrophages. Studies of $Gfi1^{-/-}$ mice showed that they were

resistant to arthritis initiated by injection of K/BxN serum, suggesting that this model of passive arthritis required neutrophils as demonstrated by antibody-mediated depletion of neutrophils.[23,30,31]

To determine whether *Genista* mice were resistant to arthritis initiated by transfer of K/BxN serum, WT, *Genista* and healthy *Gfi1*$^{-/-}$ mice were injected with K/BxN serum and the arthritis severity monitored every second day for 10 days after serum transfer. In all the WT mice, signs of arthritis were already visible at day 2 and worsened over the next 8 days (Figure 4A). As expected, *Gfi1*$^{-/-}$ mice were highly resistant to arthritis. All the *Genista* mice developed signs of arthritis at day 2 but in contrast to that observed in WT mice, arthritis in *Genista* mice did not worsen over time (Figure 4A). Considering that *Gfi1*$^{-/-}$ and *Genista* mice contained similar numbers of monocytes/macrophages and primarily differed by the presence of atypical CD11b^{+}Ly-6G^{int} neutrophils, we determined whether those last cells were responsible for the mild form of arthritis observed in *Genista* mice. Accordingly, *Genista* mice were treated with anti-Gr1 antibodies that deplete such atypical neutrophils. None of the antibody-treated *Genista* mice developed sign of arthritis upon injection of K/BxN serum (Figure 4A). Therefore, the small numbers of atypical CD11b^{+}Ly-6G^{int} neutrophils present in *Genista* mice function, to the extent that they can induce a mild arthritis in the K/BxN model of autoantibody-induced arthritis. Activated neutrophils release myeloperoxidase, the activity of which can be monitored *in vivo* using bioluminesence.[32] Bioluminescence measurements showed that myeloperoxidase activity was readily detectable in the four paws of K/BxN serum injected *Genista* mice (Figure 4B). Consistent with the mild clinical score observed in *Genista* mice, this activity was, however, four-fold reduced as compared to that of K/BxN serum injected WT mice. Altogether, these results demonstrate that the pro-inflammatory activities of the Genista neutrophils are reduced as compared to WT neutrophils.

Immune complex-mediated alveolitis in *Genista* mice

Systemic injection of ovalbumin (OVA) followed by intranasal instillation of rabbit anti-OVA serum generates immune complexes (IC) that are responsible for a type of inflammation known as alveolitis. This inflammatory reaction is characterized by a rapid influx of neutrophils that starts 4 hours post-instillation, reaches a peak between 8 and 18 hours and resolves at 72 hours, a time point at which the number of alveolar macrophages started to increase.[33] To determine whether *Genista* mice were capable of developing IC-mediated lung alveolitis, they were injected with OVA and challenged with rabbit anti-OVA serum. Progression of alveolitis was monitored at 4 hour-intervals during the first 16 hours of the reaction by analyzing BAL for the presence of neutrophils and by determining the extent of lung tissue damage, the numbers of alveolar macrophages and their capacity to produce TNF-α. As expected for WT mice, mature neutrophils started to appear at 4 hours and their numbers increased over time (Figure 5A). In contrast, in *Genista* mice, recruitment of the atypical neutrophils present in the blood was only detectable at 8 hours post-challenge and they did not accumulate over time. Analysis of *Gfi*$^{-/-}$ mice and of anti-Gr1-treated WT and *Genista* mice at 16 hours post-challenge revealed a complete absence of neutrophil influx (Figure 5A). Both WT and *Genista* mice developed a hemorrhage that increased over time (Figure 5B). However, hemorrhagic levels were significantly reduced in *Genista* mice. Consistent with the view that the early neutrophil influx increases vascular permeability and results in hemorrhage,[34] *Gfi*$^{-/-}$ mice and anti-Gr1 treated WT and *Genista* mice showed no sign of hemorrhage (Figure 5B). In contrast to WT mice that showed a sustained release of proteins in the BAL, *Genista* mice showed only a transient increase 8 hours post-challenge (Figure 5C). In all the tested mice, the number of alveolar macrophages showed no increase over the first 16 h of the reaction (Figure 5D). At 16 hours post-challenge, TNF-α was detected in the BAL of WT mice, but absent from that of *Gfi*$^{-/-}$ mice, *Genista* mice and WT mice treated with anti-Gr1 antibody (Figure 5 E). Taken together, these results showed that

the atypical Ly-6G^{int} neutrophils found in *Genista* mice were able to mount a mild IC-mediated lung alveolitis. Interestingly, *Genista* mice showed a blunted influx of neutrophils as compared to WT mice, which correlated with undetectable TNF-α production in BAL of *Genista* mice.

Mobilization of atypical neutrophils

The BM constitutes a reserve of mature neutrophils that can be mobilized in response to microbial infection.[35] Therefore, we evaluated whether the atypical end products of granulopoiesis found in *Genista* BM were capable of being mobilized after an intraperitoneal *Salmonella typhimurium* infection. Under steady state conditions, the peritoneal cavity of WT mice contained very few neutrophils. Their numbers were dramatically augmented upon *S. typhimurium* infection (Figure 6A-B). As expected, such a rapid and massive influx of neutrophils at the site of infection was accompanied by transient BM neutropenia (Figure 6A, C) and blood neutrophilia (data not shown).[36] In *Genista* mice, the steady state peritoneal cavity contained no detectable neutrophils and showed an influx of CD11b^{+}Ly-6G^{int} neutrophils after *S. typhimurium* infection (Figure 6B). As in the case of WT mice, this influx was accompanied by a reduction of the CD11b^{+}Ly-6G^{int} cell fraction present in the *Genista* BM (Figure 6A, C). Sorting of the CD11b^{+}Ly-6G^{int} cells present in the peritoneal cavity of *Genista* mice 18 hours after infection showed that, among the CD11b^{+}Ly-6G^{int} cells found in the *Genista* BM, only those with segmented nuclei were mobilized (supplemental Figure 6). Consistent with the small size of the CD11b^{+}Ly-6G^{int} cell pool found in the BM of *Genista* mice, the number of atypical neutrophils present in the peritoneal cavity of *Genista* mice 18 hours post-infection was, however, dramatically reduced compared to the number of mature neutrophils found in WT peritoneal cavity (Figure 6C). Importantly, such a reduction had a profound effect on the course of *S. typhimurium* infection, since 18 hours post-infection the peritoneal cavity of *Genista* mice contained 70-fold more *S. typhimurium* than that of WT

mice (Figure 6D). Conversely, *Genista* mice infected with *S. typhimurium* showed a normal recruitment of inflammatory monocytes that were capable of producing large amount of TNFα, IL-6, and IL-1β (Figure 6C and data not shown). Therefore, in this model, the major reduction in neutrophil influx observed in the peritoneal cavity of Genista mice had no commensurate effects on the recruitment of inflammatory monocytes. Accordingly, in the *Genista* model, the control of bacterial infection relies on effective neutrophil recruitment rather than on inflammatory monocyte recruitment.

***Genista* mice are more susceptible to infection**

To determine whether *Genista* mice had impaired resistance to acute bacterial infection, we infected them orally with *sifA*$^{-}$, an attenuated strain of *S. typhimurium.*[22] Survival of *Genista* and WT control mice that were treated or not with anti-Gr1 antibodies was monitored daily over 8 days (Figure 7 and data not shown). Whereas WT mice died between day 5 and day 8 after infection, *Genista* mice started to die as early as day 2 and were all dead by day 3, a time frame that was similar to that of antibody-treated WT mice (Figure 7). Therefore, *Genista* mice resemble neutrophil-depleted WT mice in that the small numbers of atypical CD11b^{+}Ly-6G^{int} neutrophils they posses rendered them unable to control acute bacterial infection.

Discussion

We have established and characterized *Genista*, a mouse model with a novel form of neutropenia resulting from a point mutation in the Gfi1 transcriptional repressor. The *Genista* mutation converted the cysteine residue at position 318 of the third zinc finger domain of Gfi1 into a tyrosine residue. The levels of mutated Gfi1^{C318Y} proteins expressed in *Genista* mice were comparable to the levels of Gfi1 proteins found in WT mice. Cysteine at position 318 normally is part of the Cys_2His_2 structural motif that constitutes the core component of zinc finger domains. Mutations of the amino acids that are present in zinc finger domains 3, 4 and 5 of Gfi1 are predicted to interact with DNA and revealed that mutations affecting zinc

fingers 4 and 5 had a more deleterious effects than those affecting zinc finger 3.[36-38] When kept under SPF conditions, mice homozygous for the *Genista* mutation showed normal growth and survival rates whereas *Gfi1*$^{-/-}$ mice had reduced body weight and died within the first 2-3 months of life.[11,12,14] Moreover, when compared to a *Gfi1* null mutation, the *Genista* mutation had a milder effect on hematopoietic precursors and on the development of lymphoid cells. Therefore, the *Genista* mutation likely corresponded to a partial loss of function mutation of the *Gfi1* gene. Structural studies remain, however to be performed to determine whether the *Gfi1*^{C318Y} mutation prevents the correct folding of the sole third zinc finger domain or in turn affects the organization of the adjacent zinc finger domains.

The *Genista* mutation is rather unique in that it blocked granulopoiesis just after the metamyelocytic stage and resulted in the generation of small numbers of atypical CD11b^{+}Ly-6G^{int} neutrophils. These showed a compound phenotype associating attributes characteristic of immature and of mature neutrophils. Unexpectedly, once released from the BM, this small number of atypical neutrophils was still capable of inducing some mild forms of autoantibody-induced joint inflammation and of IC-mediated lung alveolitis. The macrophages that reside in steady state tissues are thought to constitute the primary sentinels that sense invading microbes and generate pro-inflammatory cytokines. They trigger the extravasation of circulating neutrophils, which generally is followed by the recruitment of inflammatory monocytes. Studies of neutropenic patients supported the view that neutrophils are critical for the extravasation of inflammatory monocytes.[1] A recent study concluded, however, that monocytes can enter sites of infection in a manner independent of the presence of neutrophils.[39] In a model based on intraperitoneal *Salmonella typhimurium* infection, we showed that the major reduction in neutrophil influx observed in the peritoneal cavity of *Genista* mice had no commensurate effects on the recruitment of inflammatory monocytes. By analyzing the influx of myeloid cells in the peritoneal cavity of WT, *Genista* and *Gfi1*$^{-/-}$

mice 18 hours after intraperitoneal injection of thioglycollate, we showed that neutrophils were recruited in WT mice, totally absent in *Gfi1*$^{-/-}$ mice and reduced six-fold in *Genista* mice. Regardless of these marked differences in the levels of recruited neutrophils, comparable numbers of inflammatory monocytes were rapidly recruited in WT, *Genista* and *Gfi1*$^{-/-}$ mice (data not shown). Altogether, these results suggest that neutrophils are not required for the recruitment of inflammatory monocytes in the tested models.

Due to their high mortality rate, it has been difficult to determine whether the many phenotypic abnormalities displayed by *Gfi1*$^{-/-}$ mice were cell intrinsic or resulted indirectly from morbidity associated with the lack of Gfi1. In contrast, the normal viability of *Genista* mice should facilitate the studies of the complex role played by neutrophils. In conclusion, among the constellation of functions attributed to neutrophils, the novel form of neutropenia that we have characterized resulted in selective dysfunctions. For instance, whereas *Genista* mice still developed IC-mediated alveolitis and autoantibody-induced arthritis, they showed drastically impaired resistance to acute bacterial infection. The loss of control of bacterial infection in *Genista* mice is consistent with the view that normal numbers of neutrophils are crucial to control fast-replicating intracellular bacteria.[35,36,40-42] The split pattern of functional responses manifested by *Genista* mice likely reflects the distinct thresholds required for eliciting neutrophil-mediated inflammatory and anti-infectious responses. Although rare cases of severe congenital neutropenia have been associated in the human with mutation in the *GFI1* gene, none of them appear to recapitulate the conditions observed in the *Genista* mouse model.[38,43-45] It remains thus to be determined whether partial loss of function mutation in the human GFI1 transcriptional will also result into a selective spectrum of neutrophil dysfunctions.

Acknowledgements.

We thank B. Beutler, M. Guilliams, S. Henri, C. Kellenberger, H. Luche, R. Roncagalli, and for discussion and advice, R. Joly for assistance with western blot, M. Barad and A. Zouine for assistance with flow cytometry, D. Mathis and C. Benoist for K/BxN mice, T. Möröy for *Gfi1*$^{-/-}$ mice. Bioluminescence analysis was performed on Plate-forme d'Imagerie Dynamique (Institut Pasteur, Paris) and Luminex analysis at Centre d'Immunologie Humaine (Institut Pasteur, Paris).

This work was supported by Centre National de la Recherche Scientifique, Institut National de la Santé et de la Recherche Médicale, European Communities (MASTERSWITCH and MUGEN projects), GIS-IBISA-Centre d'Immunophénomique, ANR and by fellowships from FRM and ARC (D.O.-R.), from FRM (F.J.), from Institut Pasteur Bourse Roux (D.A.M.), and from China scholarship council (Y.L.).

Authorship

Contribution: D.O.-R., F.J., D.A.M., W. Z., Y.L., A.M., E.B., and P.G. performed research and analyzed data, V.B. helped designing the ENU mutagenesis screen, S.S. and M.H.d.A. performed SNP analysis, E.D. helped characterizing myeloid cells, S.M. designed the experiments involving *Salmonella* infection, P.B. designed the experiments using arthritis and alveolitis model, B.M. and M. M. designed, analyzed data and wrote the paper.

Conflict-of-interest disclosure: The authors declare no competing financial interests.

Correspondance

Marie Malissen, Centre d'Immunologie de Marseille-Luminy, Université de la Méditerranée, Case 906, 13288 Marseille Cedex 9, France.

References

1. Soehnlein O, Lindbom L. Phagocyte partnership during the onset and resolution of inflammation. *Nature reviews Immunology*. 2010;10(6):427-439.

2. Summers C, Rankin SM, Condliffe AM, Singh N, Peters AM, Chilvers ER. Neutrophil kinetics in health and disease. *Trends in immunology*. 2010;31(8):318-324.

3. Borregaard N. Neutrophils, from marrow to microbes. *Immunity*. 2010;33(5):657-670.

4. Theilgaard-Monch K, Jacobsen LC, Borup R, et al. The transcriptional program of terminal granulocytic differentiation. *Blood*. 2005;105(4):1785-1796.

5. Faurschou M, Borregaard N. Neutrophil granules and secretory vesicles in inflammation. *Microbes and Infection*. 2003;5(14):1317-1327.

6. Mantovani A, Cassatella MA, Costantini C, Jaillon S. Neutrophils in the activation and regulation of innate and adaptive immunity. *Nature reviews Immunology*. 2011;11(8):519-531.

7. Laslo P, Pongubala JM, Lancki DW, Singh H. Gene regulatory networks directing myeloid and lymphoid cell fates within the immune system. *Seminars in immunology*. 2008;20(4):228-235.

8. Moroy T, Khandanpour C. Growth factor independence 1 (Gfi1) as a regulator of lymphocyte development and activation. *Seminars in immunology*. 2011;23(5):368-378.

9. Zweidler-Mckay PA, Grimes HL, Flubacher MM, Tsichlis PN. Gfi-1 encodes a nuclear zinc finger protein that binds DNA and functions as a transcriptional repressor. *Molecular and cellular biology*. 1996;16(8):4024-4034.

10. Duan Z, Horwitz M. Gfi-1 takes center stage in hematopoietic stem cells. *Trends in molecular medicine*. 2005;11(2):49-52.

11. Hock H, Hamblen MJ, Rooke HM, et al. Intrinsic requirement for zinc finger transcription factor Gfi-1 in neutrophil differentiation. *Immunity*. 2003;18(1):109-120.

12. Karsunky H, Zeng H, Schmidt T, et al. Inflammatory reactions and severe neutropenia in mice lacking the transcriptional repressor Gfi1. *Nature genetics*. 2002;30(3):295-300.

13. Zeng H, Yucel R, Kosan C, Klein-Hitpass L, Moroy T. Transcription factor Gfi1 regulates self-renewal and engraftment of hematopoietic stem cells. *The EMBO journal*. 2004;23(20):4116-4125.

14. Yucel R, Karsunky H, Klein-Hitpass L, Moroy T. The transcriptional repressor Gfi1 affects development of early, uncommitted c-Kit+ T cell progenitors and CD4/CD8 lineage decision in the thymus. *The Journal of experimental medicine*. 2003;197(7):831-844.

15. Zhu J, Jankovic D, Grinberg A, Guo L, Paul WE. Gfi-1 plays an important role in IL-2-mediated Th2 cell expansion. *Proceedings of the National Academy of Sciences of the United States of America*. 2006;103(48):18214-18219.

16. Hock H, Orkin SH. Zinc-finger transcription factor Gfi-1: versatile regulator of lymphocytes, neutrophils and hematopoietic stem cells. *Current opinion in hematology*. 2006;13(1):1-6.

17. Kouskoff V, Korganow AS, Duchatelle V, Degott C, Benoist C, Mathis D. Organ-specific disease provoked by systemic autoimmunity. *Cell*. 1996;87(5):811-822.

18. Yucel R, Kosan C, Heyd F, Moroy T. Gfi1:green fluorescent protein knock-in mutant reveals differential expression and autoregulation of the growth factor independence 1 (Gfi1) gene during lymphocyte development. *The Journal of biological chemistry*. 2004;279(39):40906-40917.

19. Georgel P, Du X, Hoebe K, Beutler B. ENU mutagenesis in mice. *Methods in molecular biology*. 2008;415:1-16.

20. Bruhns P, Samuelsson A, Pollard JW, Ravetch JV. Colony-stimulating factor-1-dependent macrophages are responsible for IVIG protection in antibody-induced autoimmune disease. *Immunity*. 2003;18(4):573-581.

21. Jonsson F, Mancardi DA, Zhao W, et al. Human FcgammaRIIA induces anaphylactic and allergic reactions. *Blood*. 2011.

22. Henry T, Couillault C, Rockenfeller P, et al. The Salmonella effector protein PipB2 is a linker for kinesin-1. *Proceedings of the National Academy of Sciences of the United States of America*. 2006;103(36):13497-13502.

23. Monach PA, Nigrovic PA, Chen M, et al. Neutrophils in a mouse model of autoantibody-mediated arthritis: critical producers of Fc receptor gamma, the receptor for C5a, and lymphocyte function-associated antigen 1. *Arthritis and rheumatism*. 2010;62(3):753-764.

24. Voehringer D, Liang HE, Locksley RM. Homeostasis and effector function of lymphopenia-induced "memory-like" T cells in constitutively T cell-depleted mice. *Journal of immunology*. 2008;180(7):4742-4753.

25. Hardy RR, Shinton SA. Characterization of B lymphopoiesis in mouse bone marrow and spleen. *Methods in molecular biology*. 2004;271:1-24.

26. Basu S. Evaluation of role of G-CSF in the production, survival, and release of neutrophils from bone marrow into circulation. *Blood*. 2002;100(3):854-861.

27. Benarafa C, LeCuyer TE, Baumann M, Stolley JM, Cremona TP, Remold-O'Donnell E. SerpinB1 protects the mature neutrophil reserve in the bone marrow. *Journal of leukocyte biology*. 2011;90(1):21-29.

28. Pillay J, den Braber I, Vrisekoop N, et al. In vivo labeling with 2H2O reveals a human neutrophil lifespan of 5.4 days. *Blood*. 2010;116(4):625-627.

29. Kyburz D, Corr M. The KRN mouse model of inflammatory arthritis. *Springer seminars in immunopathology*. 2003;25(1):79-90.

30. Mancardi DA, Jonsson F, Iannascoli B, et al. Cutting Edge: The murine high-affinity IgG receptor FcgammaRIV is sufficient for autoantibody-induced arthritis. *Journal of immunology*. 2011;186(4):1899-1903.

31. Wipke BT, Allen PM. Essential role of neutrophils in the initiation and progression of a murine model of rheumatoid arthritis. *Journal of immunology*. 2001;167(3):1601-1608.

32. Gross S, Gammon ST, Moss BL, et al. Bioluminescence imaging of myeloperoxidase activity in vivo. *Nature medicine*. 2009;15(4):455-461.

33. Douda DN, Jackson R, Grasemann H, Palaniyar N. Innate immune collectin surfactant protein D simultaneously binds both neutrophil extracellular traps and carbohydrate ligands and promotes bacterial trapping. *Journal of immunology*. 2011;187(4):1856-1865.

34. Grommes J, Soehnlein O. Contribution of neutrophils to acute lung injury. *Molecular medicine*. 2011;17(3-4):293-307.

35. Yang KK, Dorner BG, Merkel U, et al. Neutrophil influx in response to a peritoneal infection with Salmonella is delayed in lipopolysaccharide-binding protein or CD14-deficient mice. *Journal of immunology*. 2002;169(8):4475-4480.

36. Seiler P, Aichele P, Raupach B, Odermatt B, Steinhoff U, Kaufmann SH. Rapid neutrophil response controls fast-replicating intracellular bacteria but not slow-replicating Mycobacterium tuberculosis. *The Journal of infectious diseases*. 2000;181(2):671-680.

37. Zarebski A, Velu CS, Baktula AM, et al. Mutations in growth factor independent-1 associated with human neutropenia block murine granulopoiesis through colony stimulating factor-1. *Immunity*. 2008;28(3):370-380.

38. Person RE, Li FQ, Duan Z, et al. Mutations in proto-oncogene GFI1 cause human neutropenia and target ELA2. *Nature genetics*. 2003;34(3):308-312.

39. Shi C, Pamer EG. Monocyte recruitment during infection and inflammation. *Nature reviews Immunology*. 2011;11(11):762-774.

40. Kirby AC, Yrlid U, Wick MJ. The innate immune response differs in primary and secondary Salmonella infection. *Journal of immunology*. 2002;169(8):4450-4459.

41. Vassiloyanakopoulos AP, Okamoto S, Fierer J. The crucial role of polymorphonuclear leukocytes in resistance to Salmonella dublin infections in genetically susceptible and resistant mice. *Proceedings of the National Academy of Sciences of the United States of America*. 1998;95(13):7676-7681.

42. Wick MJ. Living in the danger zone: innate immunity to Salmonella. *Current opinion in microbiology*. 2004;7(1):51-57.

43. Boztug K, Klein C. Novel genetic etiologies of severe congenital neutropenia. *Current opinion in immunology*. 2009;21(5):472-480.

44. Hochberg JC, Miron PM, Hay BN, et al. Mosaic tetraploidy and transient GFI1 mutation in a patient with severe chronic neutropenia. *Pediatric blood & cancer*. 2008;50(3):630-632.

45. Klein C. Genetic defects in severe congenital neutropenia: emerging insights into life and death of human neutrophil granulocytes. *Annual review of immunology*. 2011;29:399-413.

46. Kondo M, Weissman IL, Akashi K. Identification of clonogenic common lymphoid progenitors in mouse bone marrow. *Cell*. 1997;91(5):661-672.

47. Akashi K, Traver D, Miyamoto T, Weissman IL. A clonogenic common myeloid progenitor that gives rise to all myeloid lineages. *Nature*. 2000;404(6774):193-197.

Table 1. Absolute numbers of myeloid and lymphoid cells in the Bone Marrow (A), Thymus (B) and Spleen (C) from 6- to 8-week-old *Genista* mice and B6 control mice.

A. Bone Marrow			
• Progenitors ($x10^4$)	B6 (n=5)	*Genista* (n=5)	
HSC	2.95 ± 0.73	1.89 ± 0.22	ns
CLP	0.94 ± 0.37	0.80 ± 0.17	ns
CMP	5.31 ± 0.85	6.79 ± 04.47	ns
MEP	9.27 ± 3.06	11.8 ± 1.42	ns
GMP	7.48 ± 1.76	19.7 ± 3.18	**
• B cell precursors ($x10^6$)	B6 (n=6)	*Genista* (n=6)	
CD45R+CD43+(A/B/C)	1.09 ± 0.05	0.67 ± 0.11	**
A	0.69 ± 0.05	0.33 ± 0.06	***
B	0.26 ± 0.02	0.18 ± 0.03	ns
C	0.12 ± 0.01	0.10 ± 0.03	ns
CD45R+CD43-(D/E/F)	4.94 ± 0.60	3.85 ± 0.98	ns
• Myeloid cells ($x10^6$)	B6 (n=6)	*Genista* (n=6)	
Monocytes	2.79 ± 0.30	10.9 ± 1.20	***
Neutrophils Ly-$6G^{dim}$	1.97± 0.32	1.37 ± 0.22	ns
Neutrophils Ly-$6G^{high}$	8.90 ± 1.36	0.29 ± 0.10	****
B. Thymus ($x10^6$)	B6 (n=9)	*Genista* (n=9)	
Total cells	125.6 ± 12.7	54.9 ± 7.3	***
DN	3.52 ± 0.52	1.41 ± 0.22	**
DP	109.3 ± 12.2	47.6 ± 7.1	***
CD4 SP	7.61 ± 0.70	3.33 ± 0.42	***
CD8 SP	2.56 ± 0.26	1.05 ± 0.1	***
C Spleen ($x10^6$)	B6 (n=4-6)	*Genista* (n=4-6)	
Total cells	99.3 ± 7.6	69.5 ± 5.9	*
T cells	27.2 ± 4.3	17.6 ± 3.7	ns
CD4	14.4 ± 2.6	8.95 ± 1.7	ns
CD8	10.8 ± 1.9	7.71 ± 2.2	ns
Treg	1.09 ± 0.1	1.12 ± 0.1	ns
B cells	33.7 ± 5.9	24.9 ± 3.3	ns
NK	3.20 ± 0.65	1.69 ± 0.26	ns
Resident Monocytes	5.28 ± 1.32	3.29 ± 0.41	ns
Inflammatory Monocytes	1.85 ± 0.48	2.45 ± 1.04	ns
Neutrophils	0.30 ± 0.08	0.02 ± 0.01	*
Resident DC	0.74 ± 0.08	0.87 ± 0.03	ns
pDC	0.08 ± 0.03	0.11 ± 0.06	ns

Data are shown as mean ± SEM and number of mice analyzed is indicated (n). *P* values below 0.05 are considered to be significant. Degree of significance is indicated as follow: ns, not significant, **p,* ≤0.05, ***p*, ≤0.01, and ****p*, ≤0.001.

Figure Legends

Figure 1. Identification of *Genista* mouse mutant. (A) Percentages of neutrophils ($CD11b^+Ly\text{-}6G^+$), monocytes ($CD11b^+Ly\text{-}6G^-SSC^{low}Ly\text{-}6C^{-\text{ to }+}$) and eosinophils ($CD11b^+Ly\text{-}6^-SSC^{high}$) in the blood of B6 and *Genista* mice. Dot plots correspond to $CD5^-$ $CD19^-$ $CD161^-$ non lymphoid populations and the percentages of cells found in each of the specified gates are indicated. (B) Quantification of the data shown in (A) and in supplemental Figure 1. The specified numbers of cells per µl of blood were averaged from six, age-matched B6 and *Genista* mice that were raised in the same conditions. The absolute number of T cells, B cells, NK cells, neutrophils, monocytes and eosinophils per μl of blood was calculated as specified in supplemental Figure 1 using the formula: Cell counts / Bead counts x Total Trucount bead / μl of blood. The error bars correspond to the SEM. *, $p \leq 0.05$, ***, $p \leq 0.001$. Data are representative of 3 independent experiments. (C) Comparison of the expression of Ly-6G on the $CD11b^+$ cells found in the blood of WT, *Genista* and *Gfi1*$^{-/-}$ mice. The percentages of cells found in each of the specified gates are indicated. Data are representative of two independent experiments. (D) The *Genista* mutation does not affect Gfi1 expression. Expression of Gfi1 in thymocytes from WT, *Genista* and *Gfi1*$^{-/-}$ mice was detected by Western blotting. The position of the band corresponding to Gfi1 (55 kDa) is shown. Probing with a monoclonal antibody against α-tubulin demonstrates that each lane was loaded with comparable amounts of material.

Figure 2. Genetic mapping and identification of the *Genista* mutation. (A) The *Genista* mutation was mapped by outcrossing the B6 mutant stock to C3HeB/FeJ (C3H) mice and by subsequent brother-sister mating. 46 neutropenic mice were identified among the offsprings and their DNA analyzed using a panel of 153 SNP markers. The strongest linkage corresponding to a -log10(P) value of 10.71 was associated with SNP rs32067291 at position

111.71 Mb of chromosome 5. The highest -log10(P) value of each individual chromosome is also shown. Map coordinates refer to the Ensembl public mouse genome assembly (http://mouse.ensembl..org/) (B) High-resolution mapping of informative mice using 8 additional SNP markers confined the *Genista* mutation to the 106.2-124.91 Mb interval of chromosome 5. Grey and white rectangles correspond to intervals with a homozygous (C57BL/6) or heterozygous (C57BL/6 x C3H) status, respectively. The number of mice corresponding to each of the 5 identified genotypes is indicated on the left. (C) Comparison of the sequence of the *Gfi1* gene from C57BL/6 control mice, heterozygous *Gfi1*$^{Gen/+}$ and homozygous *Gfi1*$^{Gen/Gen}$ mice revealed a G → A transition (arrow) at position 5557 bp of the Gfi1-001 transcript (ENSMUST00000159164, http://www.ensembl.org). (D) Schematic representation of the Gfi1 protein with the amino-terminal SNAG domain (grey) and the 6 C_2H_2-type zinc finger domains (pink). The *Genista* mutation converts the cysteine (C) residue found at position 318 of the third zinc finger domain into a tyrosine (Y). (E) Sequence alignment of the third zinc finger domain encoded by the C57BL/6 and *Genista* alleles of the *Gfi1* gene, and schematic representation of the third C_2H_2-type zinc finger domain. The zinc ion (orange) is coordinated by two histidine residues (green) and two cysteine residues (red). The C → Y substitution affects the second cysteine of the Cys_2His_2 core structural motif.

Figure 3. *Genista* mice lack mature Ly-6G^{high} neutrophils. (A) Analysis of BM cells of WT and *Genista* mice for CD11b and Ly-6G. Gates corresponding to CD11b$^+$Ly-6G^{int} and CD11b$^+$Ly-6G^{high} neutrophils were defined based on staining of WT BM cells. The percentages of cells found in each of the specified gates are indicated. (B) Absolute numbers of Ly-6G^{int} and Ly-6G^{high} neutrophils and of Ly-6C$^+$ monocytes in BM isolated from WT (open bars) and *Genista* (filled bars) femurs and tibias. Data were averaged from six WT and six *Genista* mice at 6 to 9 weeks of age. The error bars correspond to the SEM. ***; $p < 0.001$. (C) Morphological characteristics of Ly-6G^{int} and Ly-6G^{high} neutrophils sorted from WT and

Genista BM, analyzed by Wright-Giemsa staining after cytospin onto glass slides. Total BM cells (Total) are also shown. Black arrows indicate metamyelocytes and pink ones segmented nuclei neutrophils. Magnification: 63X (D) Lineage$^-$ (CD3$^-$CD19$^-$CD161$^-$Ter119$^-$) CD11b$^-$ Ly-6G$^-$ cells containing the earliest stages of granulopoiesis (CD11b$^-$ precursors), Ly-6G^{int} and Ly-6G^{high} neutrophils were sorted from the BM of WT (open bars) and *Genista* (filled bars) mice. RNA was prepared from each sample and analyzed by quantitative RT-PCR for the expression of *Mpo*, *Ltf* and *Mmp9* transcripts. Results are expressed as relative units of *Mpo*, *Ltf* and *Mmp9* mRNA normalized using *Hprt* transcript and averaged from 4 independent experiments. The error bars correspond to the SEM. (E) Kinetics of BrdU-labelling of immature (Ly-6G^{int}) and mature (Ly-6G^{high}) neutrophils present in the BM of WT mice (top panels) and of immature neutrophils (Ly-6G^{int}) present in *Genista* mice (bottom panels). Mice were exposed to BrdU and the percentages of BrdU$^+$ cells and the absolute number of BrdU$^+$ cells/femur determined. Five mice were analyzed per time points. Errors bars correspond to the SEM. Data are representative of two independent experiments.

Figure 4. Mild autoantibody-induced arthritis in *Genista* mice. *Genista*, WT, and *Gfi1*$^{-/-}$ mice were injected i.v. with serum from K/BxN mice (day 0). (A) When specified (+ anti-Gr1), *Genista* and WT mice were also injected with 500 µg of anti-Gr1 antibody (RB6-8C5) at day -1, 1, 2, 4 6 and 8. Clinical scores were evaluated. Mean values between WT and *Genista* mice and *Genista* mice and *Gfi1*$^{-/-}$ are highly significant (*p* value calculated for day 6 is shown, ***p*, ≤0.01). (B) Photon emission corresponding to luminol degradation by myeloperoxidase activity present in the joints was measured 5 days after injection of K/BxN serum. Bioluminescence is expressed as cumulated average radiance of the four paws. Data in (A) and (B) are representative of two independent experiments involving 4-6 animals per genotype. Error bars correspond to the SEM, ****p*, ≤0.001, and ***p*, ≤0.01.

Figure 5. Mild immune complex-mediated lung alveolitis in *Genista* mice. *Genista,* WT

and *Gfi1*$^{-/-}$ mice were injected i.v. with OVA and challenged intranasally with rabbit anti-OVA serum. When specified (+ anti-Gr1), mice were also injected with 300 μg of anti-Gr1 antibodies 24 hours before challenge. BALs were performed at the specified time points. *Gfi1*$^{-/-}$ mice were only analyzed at time points 0 and 18 hours. (A) Numbers of neutrophils in BAL. (B) Hemorrhage in BAL. (C) Concentration of total proteins in BAL. (D) Numbers of alveolar macrophages in BAL. (E) Concentration of TNF-α in BAL. Data are representative of 2 independent experiments involving 3-4 animals per genotype, except for the WT + anti-Gr1 where a single animal was evaluated. Dotted lines indicate the detection limit, N.D. no measurement done.

Figure 6. Mobilization of BM neutrophils. *S. typhimurium* were injected i.p. in WT and *Genista* mice. The BM and peritoneal cavity (PC) were analyzed for their content of neutrophils and monocytes prior to (T0) or 18 h (T18) after bacterial injection. (A-B) Analysis of the cells found in the BM and peritoneal cavity of B6 (A) and *Genista* (B) mice for CD11b and Ly-6G expression. In BM samples, the gates corresponding to mature (CD11b^{+}Ly-6G^{high}), immature (CD11b^{+}Ly-6G^{int}) neutrophils and to monocytes (CD11b^{+}Ly-6G^{-}) were defined based on staining of WT BM cells. In the case of peritoneal cavity cells, the gate corresponding to Ly-6G^{+} neutrophils was defined based on staining of B6 mice. The percentages of cells found in each of the specified gates are indicated. (C) Quantification of the data shown in (A). (D) Number of *S. typhimurium* present in the peritoneal cavity of WT and *Genista* mice 18 hours after infection. The values corresponding to each individual mouse are shown and the mean and SEM is indicated for each condition (n = 5-8).

Figure 7. *Genista* mice are more susceptible to microbial infection. *Genista* and WT mice were infected orally with *S. typhimurium sifA*$^{-}$. The percent survival is shown over a period of 8 days. When specified (+ anti-Gr1), mice were treated with anti-Gr1 antibody at day -1 and 2. Data correspond to 4 mice per group. One experiment out of two is shown.

Supplemental data

Supplemental Figures

Figure S1. Multiparameter flow cytometry analysis of blood samples of B6 and *Genista* mice. Blood was collected from the retro-orbital sinus of sedated mice using heparinized microhematocrit tubes. Staining was performed on 30 μl of whole blood using Trucount tubes (BD Biosciences) and a combination of 6 antibodies consisting of PerCP-Cy5.5 conjugated anti-CD45.2 (104), Pacific Blue conjugated anti-CD4 (RM4-5), Pacific Blue conjugated anti-CD8α (53.6.7), APC-H7 conjugated anti-CD19 (1D3/6D5), APC conjugated anti-CD161 (PK136), PE-Cy7 conjugated anti-Gr1 (RB6-8C5). Further analysis included Pacific Blue conjugated anti-CD11b (MI/70), PE conjugated anti-Ly-6G (1A8), FITC conjugated anti-Ly-6C (AL-21) and APC conjugated anti-CD5, CD19 and CD161, all from BD Biosciences. A lyse/no-wash procedure was performed using a BD FACS lysing solution (BD Biosciences). For each sample, a minimum of 30 000 $CD45.2^+$ cells were acquired using a BD FACSCanto II. Histograms showed the percentages of $CD45.2^+$ white bood cells (R1 gate) and of Trucount beads (peak at the extreme right). Among $CD45.2^+$ white blood cells, αβ T cells ($CD4^+$ or $CD8^+$), B cells ($CD19^+$), neutrophils ($CD4^-CD8^-CD19^-CD161^-Gr1^+$), NK cells ($CD4^-CD8^-CD19^-Gr1^-CD161^+$), monocytes ($CD4^-CD8^-CD19^-CD161^-Gr1^-SSC^{low}$), and eosinophils ($CD4^-CD8^-CD19^-CD161^-Gr1^-SSC^{high}$) cells were identified. The percentages of cells found in each of the specified gates are indicated.

Figure S2. T cell development in *Genista* mice. (A) Expression of CD4 and CD8 on total thymocytes and on the T cells found in the spleen of WT and *Genista* mice. (B) Expression of CD44 and CD62L on the CD4+ and CD8+ T cells found in the spleen of WT and *Genista* mice. The percentages of cells found in each of the specified gates are indicated. Data are representative of 3 independent experiments involving 6 WT and 6 *Genista* mice.

Figure S3. Effect of the *Genista* mutation on adult BM hematopoietic progenitors. (A)

Lineage negative progenitors were enriched from *Genista* and B6 BM using a Lineage Cell depletion Kit (Miltenyi Biotec). Lin^- cells were analyzed for c-kit (CD117), Sca1 and IL-7Rα (CD127) expression, allowing the identification of HSC ($Lin^-Sca1^+c\text{-}kit^+$) and CLP ($LinSca1^{low}c\text{-}kit^{low}IL7R^+$) as described in Ref 46. The $Lin^-Sca1^-c\text{-}Kit^+$ fraction was further analyzed for CD34 and CD16/32 expression to define CMPs ($CD16/32^{low}CD34^+$), GMPs ($CD16/32^{high}CD34^+$) and MEPs ($CD16/32^{low}CD34^-$) as previously described.[47] (B) Absolute numbers of HSCs, CLPs, CMPs, MEPs and GMPs per mouse of the specified genotype. Data are representative of 2 independent experiments involving 5 mice per genotype. The error bars correspond to the SEM.

Figure S4. HSCs from *Genista* mice showed a compromised reconstitution capacity. $CD45.2^+$ BM cells (3×10^6) isolated from B6 and *Genista* mice were injected into lethally irradiated $CD45.1^+$ recipient mice. 8 weeks after reconstitution, the absolute number of the specified cells was determined. (A) Numbers of $CD45.2^+$ cells in BM, thymus and spleen. (B) Numbers of DN, DP, $CD4^+$ and $CD8^+$ SP cells found in the thymus. (C) Numbers of monocytes, $Ly\text{-}6G^{int}$ and $Ly\text{-}6G^{high}$ neutrophils, and of pre- and pro-B cells present in the BM. (D) Numbers of $CD4^+$ and $CD8^+$ T cells, B cells, monocytes and neutrophils present in the spleen. Data are representative of two independent experiments involving five B6 and seven *Genista* mice. The error bars correspond to the SEM.

Figure S5. Comparison of *Genista* and *Gfi1*$^{-/-}$ mice. BM cells isolated from WT, *Genista* and *Gfi1*$^{-/-}$ mice were analyzed for CD11b and Ly-6G expression. Gates corresponding to mature ($CD11b^+Ly\text{-}6G^{high}$) and immature ($CD11b^+Ly\text{-}6G^{int}$) neutrophils and to monocytes ($CD11b^+$ $Ly\text{-}6G^-Ly\text{-}6C^+$) were defined based on staining of WT BM cells. Compared to WT neutrophils, the small percentages of neutrophils that were present in *Genista* mice expressed lower levels of Ly-6G that barely merged in the into the gates used to define $Ly\text{-}6C^{high}$ WT neutrophils. The percentages of cells found in each of the specified gates are indicated. Data

correspond to two WT and two *Gfi1*$^{-/-}$ mice.

Figure S6. Neutrophils recruited in the peritoneal cavity of Genista mice following inflammation have a mature morphology. Morphological characteristics of total cells and of sorted CD11b+Ly-6G+ neutrophils from the peritoneal cavity of WT and *Genista* following inflammation. Cells were analyzed by Wright-Giemsa staining after cytospin onto glass slides. Magnification: 63x.

Figure 1

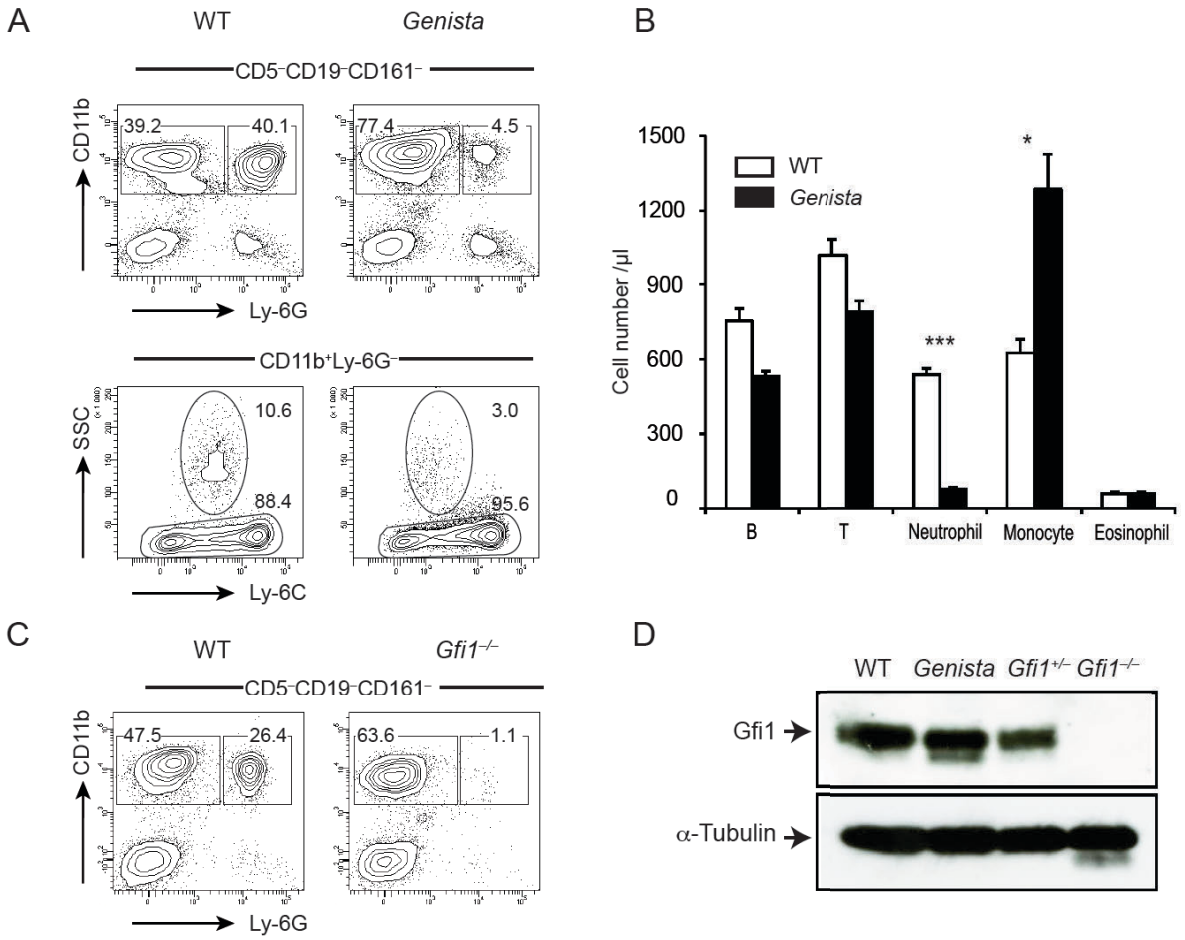
A
WT
Genista
CD5⁻CD19⁻CD161⁻
CD11b
39.2
40.1
77.4
4.5
Ly-6G
CD11b⁺Ly-6G⁻
SSC
10.6
88.4
3.0
95.6
Ly-6C
B
1500
1200
900
600
300
0
Cell number /μl
WT
Genista
***
*
B
T
Neutrophil
Monocyte
Eosinophil
C
WT
Gfi1⁻/⁻
CD5⁻CD19⁻CD161⁻
CD11b
47.5
26.4
63.6
1.1
Ly-6G
D
WT
Genista
Gfi1⁺/⁻
Gfi1⁻/⁻
Gfi1
α-Tubulin

Figure 2

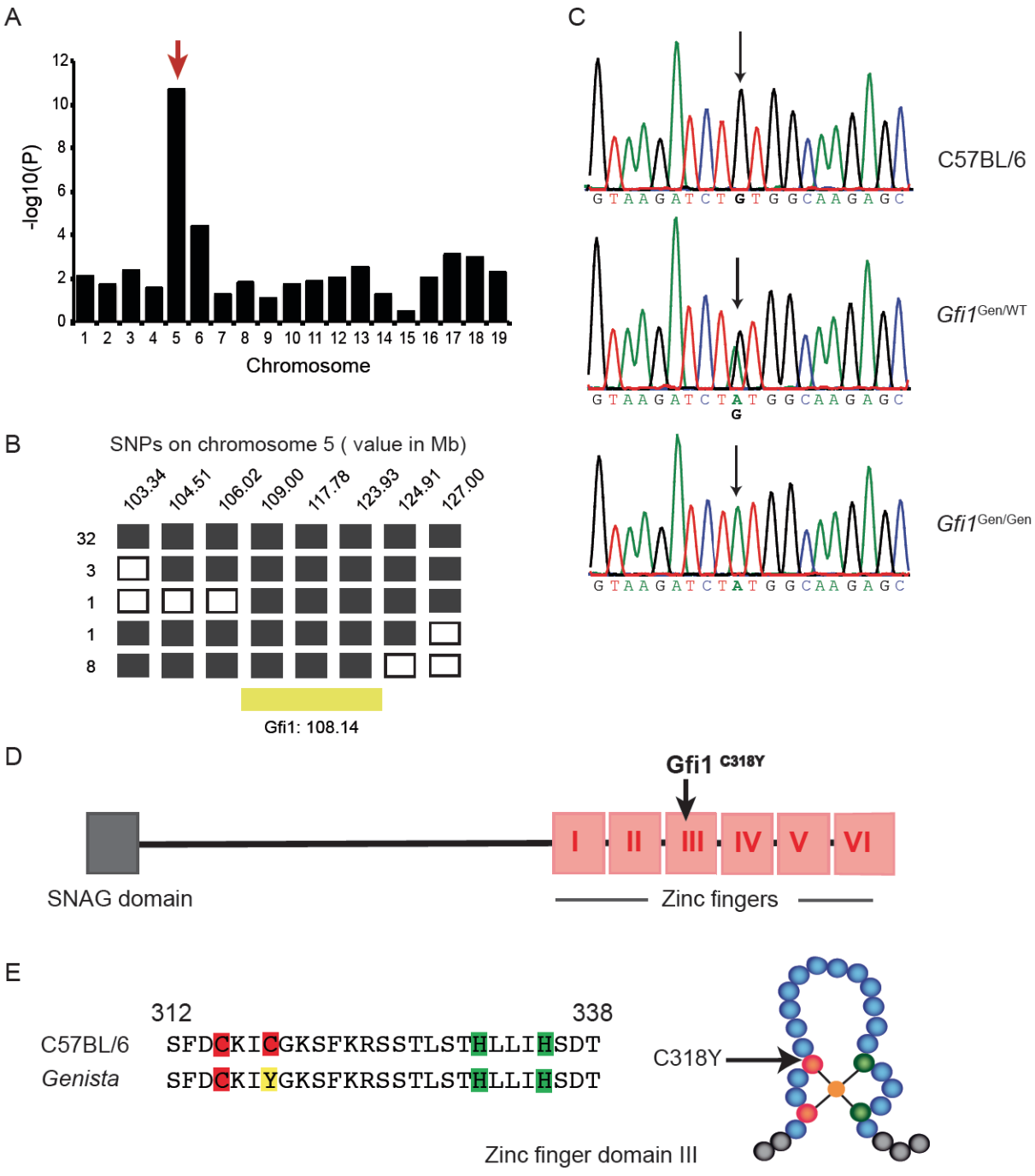
A
-log10(P)
Chromosome
B
SNPs on chromosome 5 (value in Mb)
103.34
104.51
106.02
109.00
117.78
123.93
124.91
127.00
Gfi1: 108.14
C
C57BL/6
Gfi1Gen/WT
Gfi1Gen/Gen
D
Gfi1 C318Y
SNAG domain
Zinc fingers
E
312
338
C57BL/6 SFDCKICGKSFKRSSTLSTHLLIHSDT
Genista SFDCKIYGKSFKRSSTLSTHLLIHSDT
C318Y
Zinc finger domain III

Figure 3

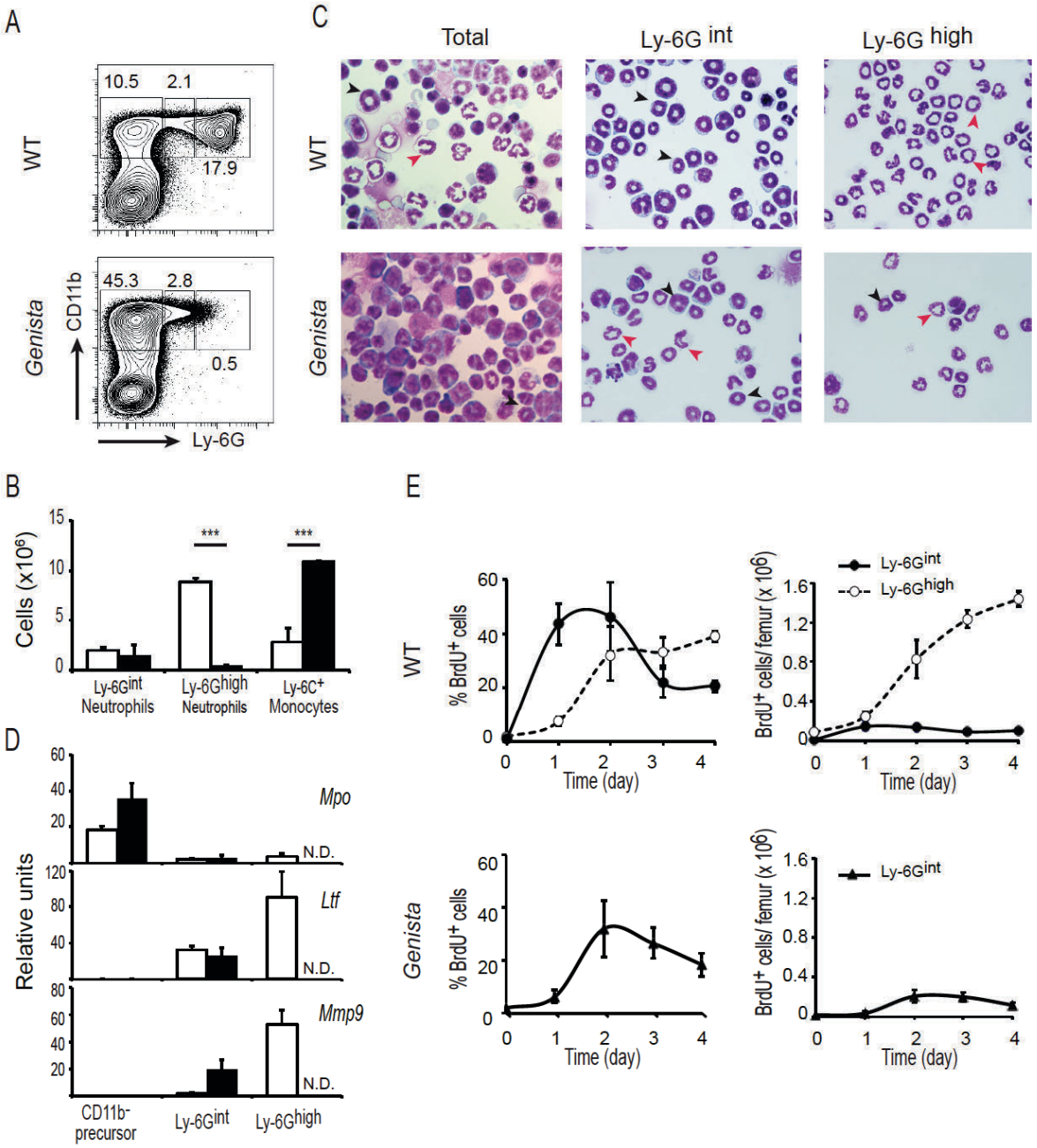
A
WT
10.5
2.1
17.9
Genista
CD11b
45.3
2.8
0.5
Ly-6G
C
Total
Ly-6G int
Ly-6G high
WT
Genista
B
Cells (x10⁶)
***
***
Ly-6G^int Neutrophils
Ly-6G^high Neutrophils
Ly-6C^+ Monocytes
D
Relative units
Mpo
N.D.
Ltf
N.D.
Mmp9
N.D.
CD11b⁻ precursor
Ly-6G^int
Ly-6G^high
E
WT
% BrdU⁺ cells
Time (day)
BrdU⁺ cells/ femur (x 10⁶)
Ly-6G^int
Ly-6G^high
Time (day)
Genista
% BrdU⁺ cells
Time (day)
BrdU⁺ cells/ femur (x 10⁶)
Ly-6G^int
Time (day)

Figure 4

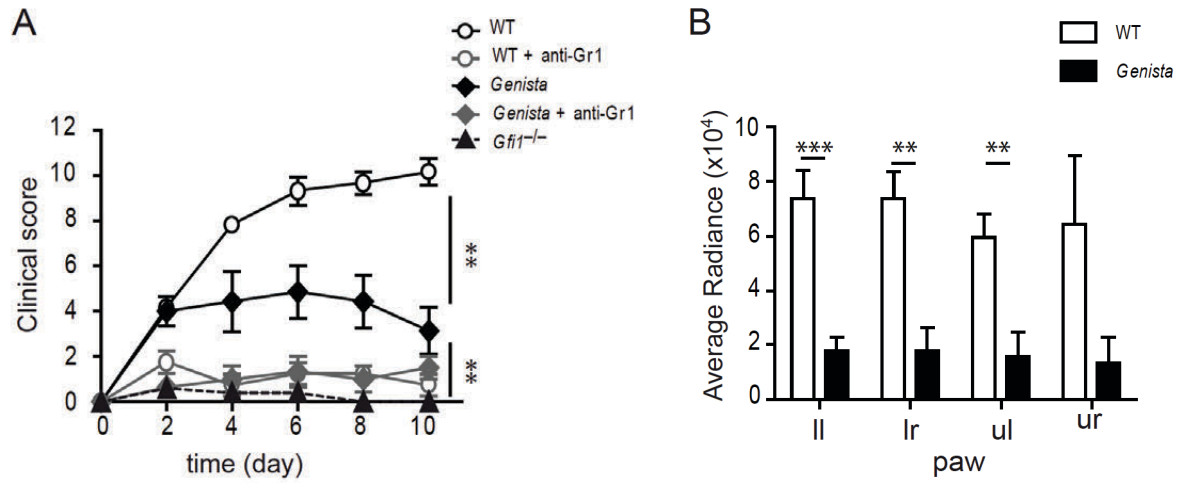
A
WT
WT + anti-Gr1
Genista
Genista + anti-Gr1
Gfi1−/−
Clinical score
time (day)
**
**
B
WT
Genista
Average Radiance (x10⁴)
***
**
**
ll
lr
ul
ur
paw

Figure 5

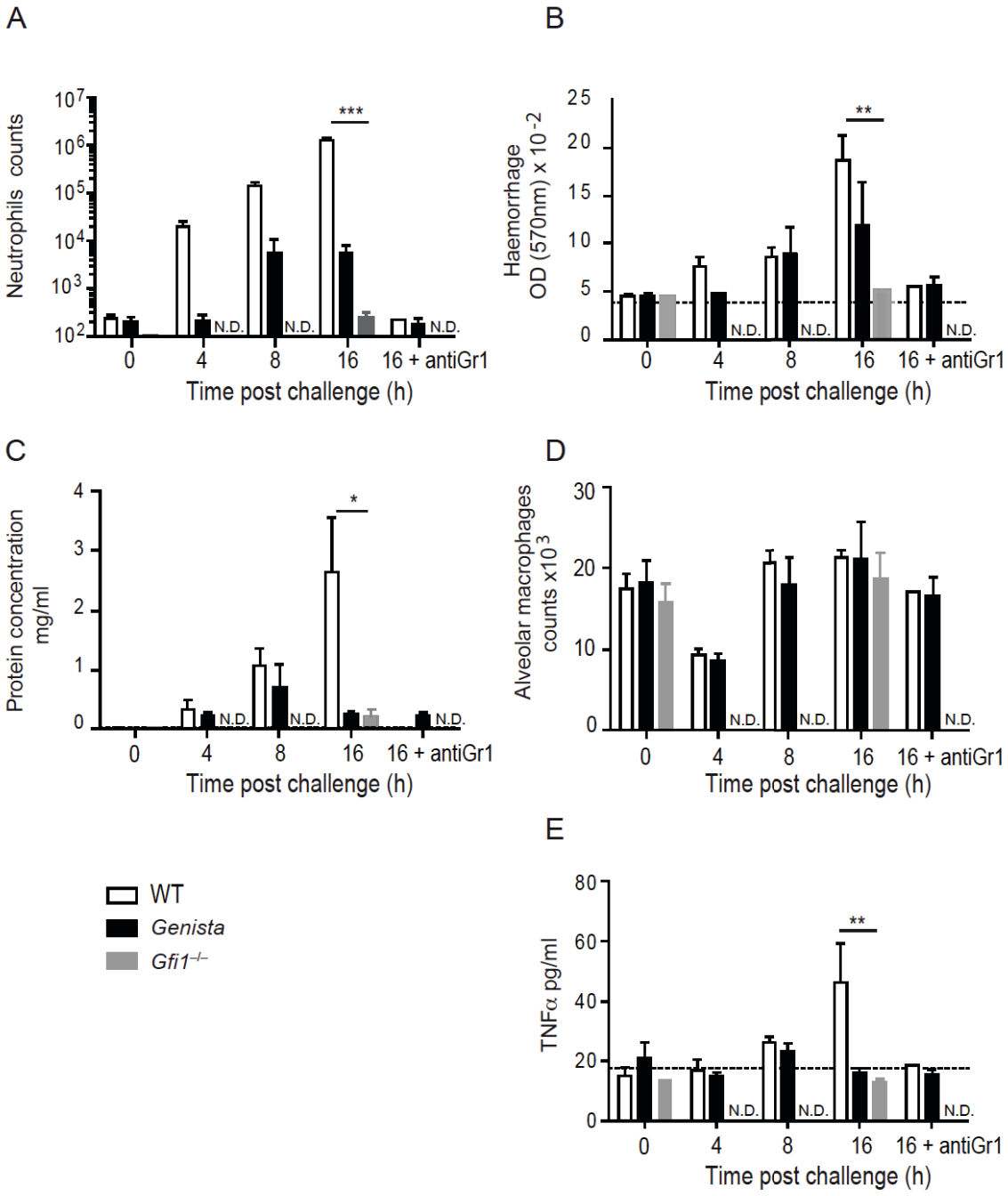
A
Neutrophils counts
10^7
10^6
10^5
10^4
10^3
10^2
***
N.D.
N.D.
N.D.
0
4
8
16
16 + antiGr1
Time post challenge (h)
B
Haemorrhage
OD (570nm) x 10^{-2}
25
20
15
10
5
0
**
N.D.
N.D.
N.D.
0
4
8
16
16 + antiGr1
Time post challenge (h)
C
Protein concentration
mg/ml
4
3
2
1
0
*
N.D.
N.D.
N.D.
0
4
8
16
16 + antiGr1
Time post challenge (h)
D
Alveolar macrophages
counts x10^3
30
20
10
0
N.D.
N.D.
N.D.
0
4
8
16
16 + antiGr1
Time post challenge (h)
WT
Genista
Gfi1-/-
E
TNFα pg/ml
80
60
40
20
0
**
N.D.
N.D.
N.D.
0
4
8
16
16 + antiGr1
Time post challenge (h)

Figure 6

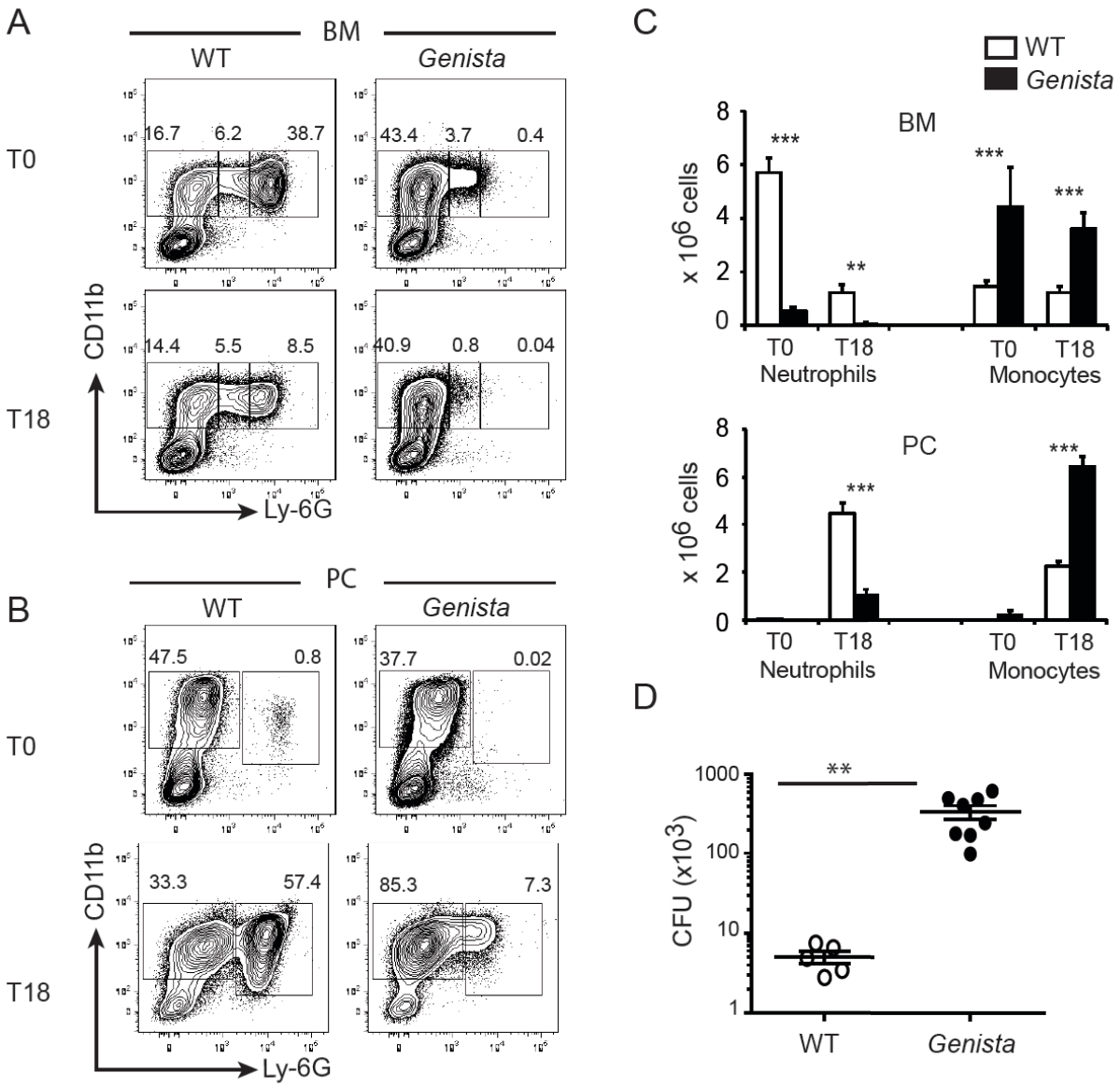
A
BM
WT
Genista
T0
T18
16.7
6.2
38.7
43.4
3.7
0.4
14.4
5.5
8.5
40.9
0.8
0.04
CD11b
Ly-6G
B
PC
WT
Genista
T0
T18
47.5
0.8
37.7
0.02
33.3
57.4
85.3
7.3
CD11b
Ly-6G
C
WT
Genista
BM
x 10^6 cells
***
**
***
***
T0
T18
T0
T18
Neutrophils
Monocytes
PC
x 10^6 cells
***
***
T0
T18
T0
T18
Neutrophils
Monocytes
D
CFU (x10^3)
**
1000
100
10
1
WT
Genista

Figure 7

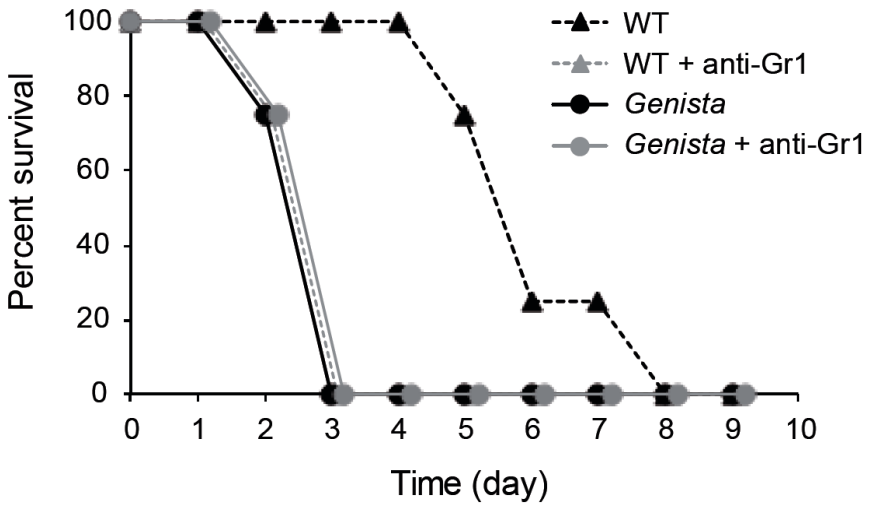
Percent survival
100
80
60
40
20
0
0
1
2
3
4
5
6
7
8
9
10
Time (day)
WT
WT + anti-Gr1
Genista
Genista + anti-Gr1

Figure S1

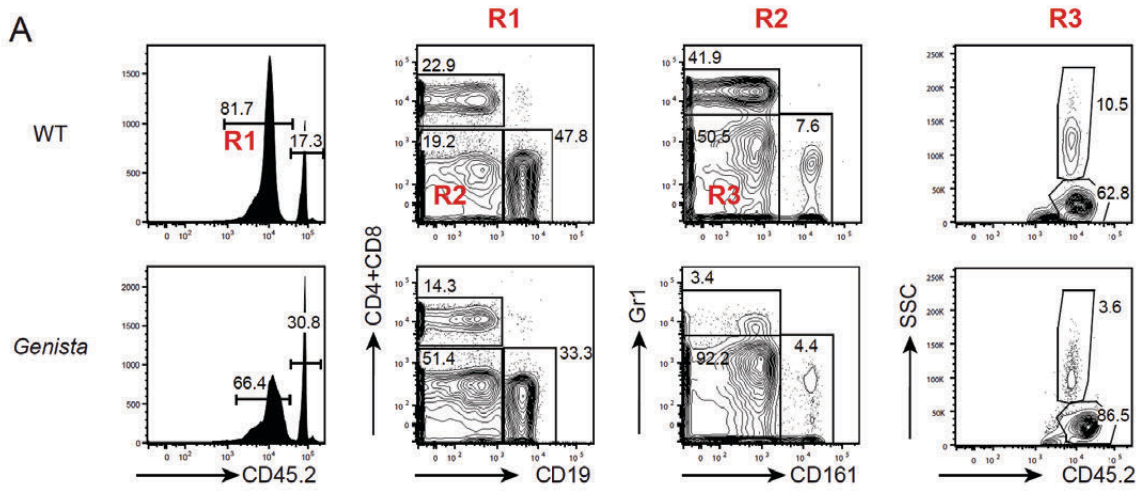
A
R1
R2
R3
WT
Genista
81.7
R1
17.3
30.8
66.4
CD45.2
22.9
19.2
R2
47.8
14.3
51.4
33.3
CD4+CD8
CD19
41.9
50.5
R3
7.6
3.4
92.2
4.4
Gr1
CD161
10.5
62.8
3.6
86.5
SSC
CD45.2

Figure S2

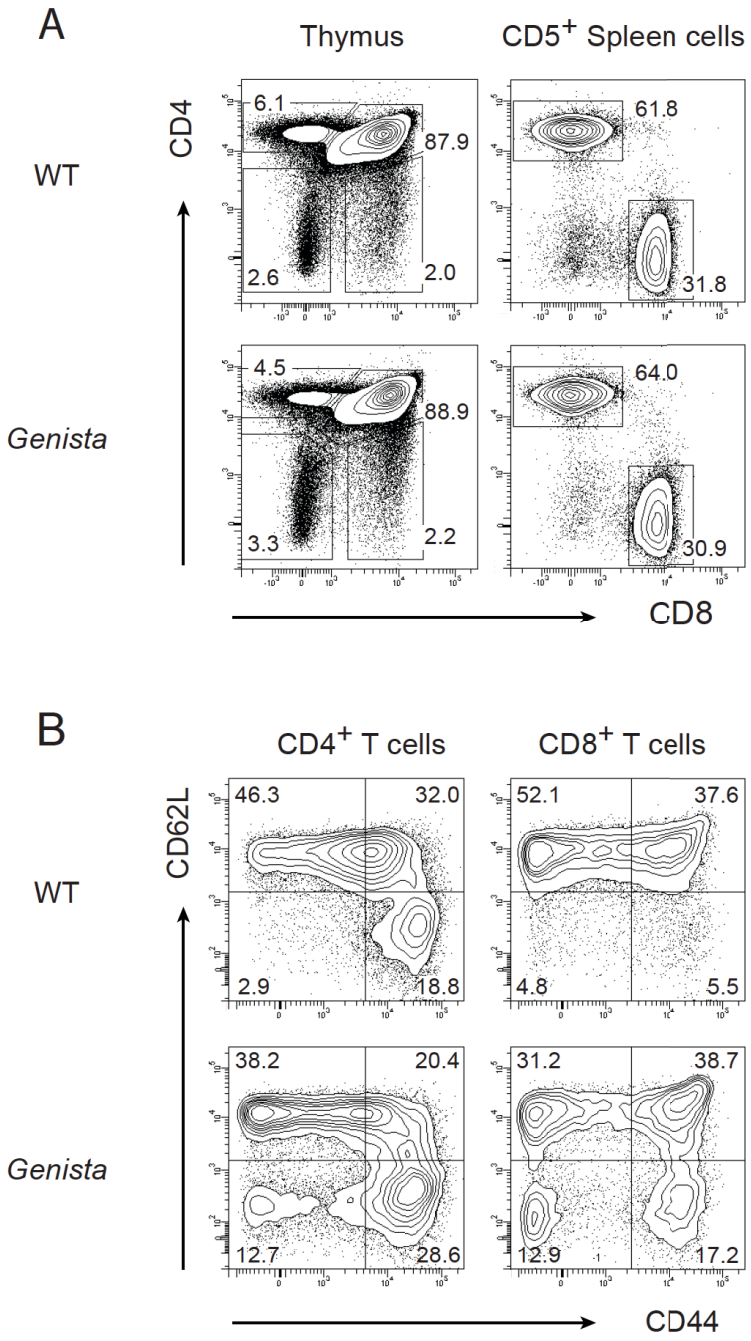
A
Thymus
CD5+ Spleen cells
WT
Genista
CD4
CD8
6.1
87.9
2.6
2.0
61.8
31.8
4.5
88.9
3.3
2.2
64.0
30.9
B
CD4+ T cells
CD8+ T cells
WT
Genista
CD62L
CD44
46.3
32.0
2.9
18.8
52.1
37.6
4.8
5.5
38.2
20.4
12.7
28.6
31.2
38.7
12.9
17.2

Figure S3

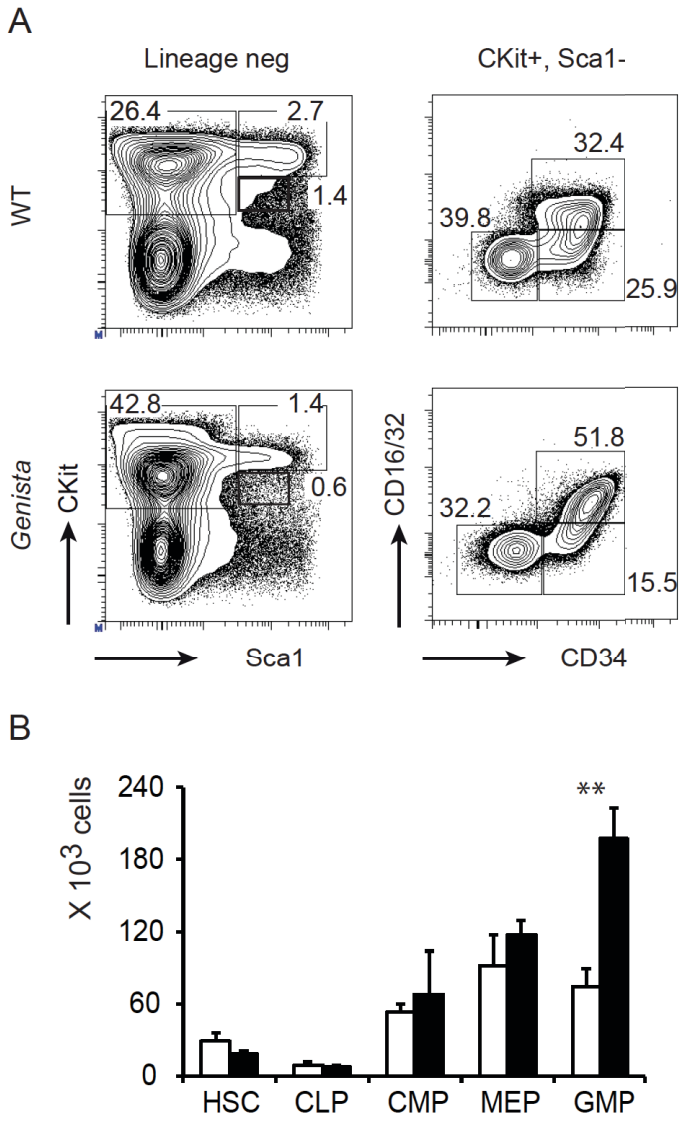
A
Lineage neg
CKit+, Sca1-
WT
Genista
26.4
2.7
1.4
32.4
39.8
25.9
42.8
1.4
0.6
51.8
32.2
15.5
CKit
Sca1
CD16/32
CD34
B
X 10^3 cells
240
180
120
60
0
**
HSC
CLP
CMP
MEP
GMP

Figure S4

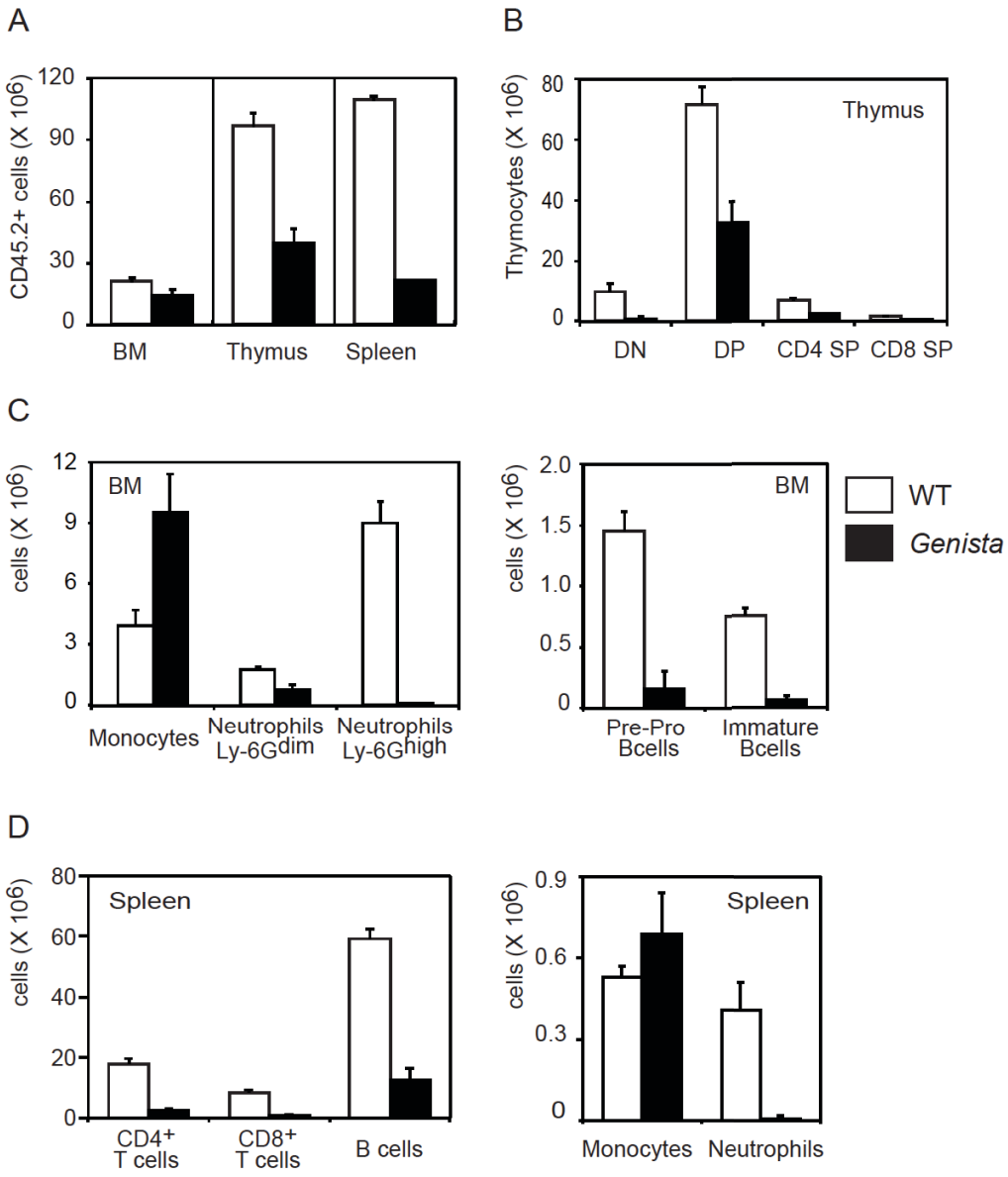
A
CD45.2+ cells (X 10⁶)
120
90
60
30
0
BM
Thymus
Spleen
B
Thymocytes (X 10⁶)
80
60
40
20
0
Thymus
DN
DP
CD4 SP
CD8 SP
C
cells (X 10⁶)
12
9
6
3
0
BM
Monocytes
Neutrophils Ly-6G^dim
Neutrophils Ly-6G^high
cells (X 10⁶)
2.0
1.5
1.0
0.5
0
BM
Pre-Pro Bcells
Immature Bcells
WT
Genista
D
cells (X 10⁶)
80
60
40
20
0
Spleen
CD4⁺ T cells
CD8⁺ T cells
B cells
cells (X 10⁶)
0.9
0.6
0.3
0
Spleen
Monocytes
Neutrophils

Figure S5

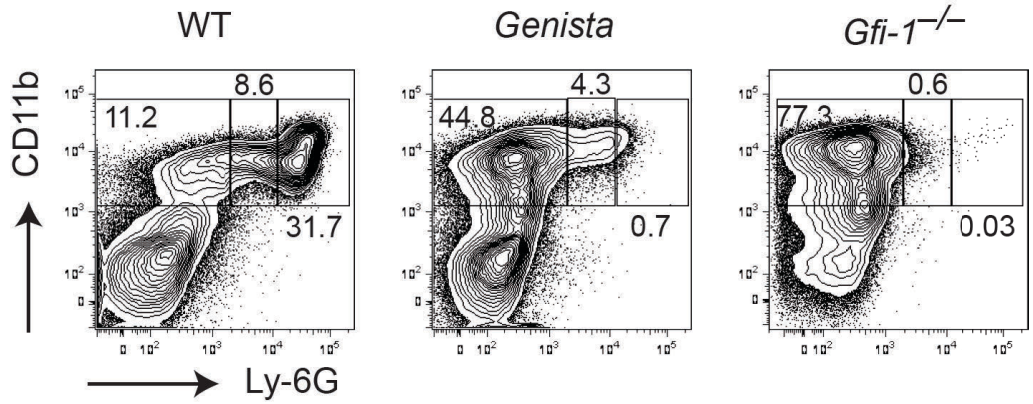

Figure S6